



Apostolos KYRITSIS

**Micro and Nanotechnologies for Integrated Systems
2021**

**CSEM : Rue Jacquet-Droz 1, 2002 Neuchâtel, Switzerland
EPFL: Rte Cantonale, 1015 Lausanne, Switzerland**

Chemical Sensing with Ion-Sensitive Field-Effect Transistors

from 15/02/21 to 13/08/21

Confidentiality: no

Under the supervision of:

- **CSEM supervisor: Nicholas HENDRICKS,
nicholas.hendricks@csem.ch**

Present at the defense: yes

- **EPFL supervisor: Adrian IONESCU, adrian.ionescu@epfl.ch**

-

Present at the defense: no

- **Phelma Tutor: Irina IONICA, Irina.Ionica@phelma.grenoble-inp.fr**

**Ecole nationale
supérieure de physique,
électronique, matériaux**

Phelma

Bât. Grenoble INP - Minatec
3 Parvis Louis Néel - CS 50257
F-38016 Grenoble Cedex 01

Tél +33 (0)4 56 52 91 00
Fax +33 (0)4 56 52 91 03

<http://phelma.grenoble-inp.fr>

Table of Contents

Table of Contents	3
Glossary	4
List of Figures	5
List of Tables.....	6
1. Introduction.....	7
1.1 History and Importance of pH Sensing	7
1.2 Overview of the Internship	7
1.3 Description of the Sites.....	8
2. The Ion-Sensitive Field-Effect Transistor (ISFET)	9
2.1 The pH Scale	9
2.2 Working Principles	9
2.3 The Reference Electrode	12
2.4 ISFET Development Process at CSEM	13
3. Packaging	15
3.1 Criteria and Challenges	15
3.2 Preparation of the Epoxy	15
3.3 Wire Bonding	16
3.4 Fine Encapsulation	17
3.5 Main Body Encapsulation	17
4. Characterization of the ISFET	19
4.1 Measurement Setup	19
4.2 Burn-in Response and Reproducibility.....	20
4.3 Measuring Sensitivity	24
4.4 Temperature Dependence	25
4.5 The Isothermal Point	26
4.6 Long-Term Voltage Drift	27
4.7 Hysteresis.....	28
5. Testing ISFETs for Biological Applications.....	30
5.1 Overview.....	30
5.2 Bio-Compatibility of the ISFET	30
6. Sensing Layer with ALD	33
6.1 Overview of the Gate Structure.....	33

6.2	Construction of the EIS	33
6.3	Characterization	37
7.	Ion-Selective Membrane	39
7.1	Overview	39
7.2	Aerosol Jet Printing	39
7.3	Results	41
8.	Conclusions.....	42
9.	Bibliography	43
Annex	45
	Description of Sites.....	45
	Project Schedule (Gantt Diagram).....	46
	Summary	47

Glossary

<i>ALD</i>	Atomic Layer Deposition
<i>CMi</i>	Center of MicroNanoTechnology
<i>CSEM</i>	Swiss Center for Electronics and Microtechnology
<i>EIS</i>	Electrolyte-Insulator-Semiconductor
<i>EPFL</i>	École Polytechnique Fédérale de Lausanne
<i>H₂O</i>	Water
<i>H₃O⁺</i>	Hydronium
<i>HfO₂</i>	Hafnium Oxide
<i>ISFET</i>	Ion-Selective Field-Effect Transistor
<i>LPCVD</i>	Low-Pressure Chemical-Vapor-Deposition
<i>MOSFET</i>	Metal-Oxide-Semiconductor Field Effect Transistor
<i>NANOLAB</i>	Laboratory of Micro/Nanoelectronic Devices
<i>NH₃</i>	Ammonia
<i>NH₄</i>	Ammonium Cation
<i>OH⁻</i>	Hydroxide
<i>SiO₂</i>	Silicon Dioxide
<i>Ta₂O₅</i>	Tantalum Oxide

List of Figures

Figure 1 : On the left is a simplified overview of a MOSFET. On the right, a simplified overview of the ISFET produced at CSEM. The gate electrode of the MOSFET is replaced by the solution as well as the reference electrode.	10
Figure 2: Oxide surface / electrolyte interface. The oxide surface is coated with sites of OH groups that interact with the solution.	11
Figure 3 : The double junction reference electrode reference electrode.	12
Figure 4: Gate stack layers produced by CSEM. The thicknesses might vary slightly from chip to chip.	13
Figure 5 : A diced 100mm wafer for the fabrication of 218 ISFET chips (left). On the right is an image of a single ISFET. Both Source and Drain contacts are visible, and there are also 2 more contacts for a diode that can be used as a temperature sensor.	14
Figure 6 : A closeup of the gate under an optical Microscope. The encircled geometry must always be exposed to be in contact with the solution.	14
Figure 7 : Epoxy on the PCB without using Thinky Mixer (left). Epoxy on another PCB with 4 continuous minutes of mixing with the Thinky Mixer (right).	16
Figure 8 : Wire bonder machine (left), The wire bonded ISFET chip (right).	16
Figure 9: A closeup of the encapsulated sensor. The gate in the middle is clearly exposed. ..	16
Figure 10: Image of an encapsulated ISFET.	18
Figure 11 :The overview of the ISFET measurement setup.	19
Figure 12 : ISFET amplifier. On the top right screen, the amount of leakage current detected from all the active ISFETs. On the display below, the output voltage is displayed depending on which channel is selected.	19
Figure 13: This graph shows the burn-in curves of a single ISFET submerged 3 times in pH 1 solution.	21
Figure 14: This graph shows the burn-in curves of a single ISFET submerged 3 times in pH 4 solution.	21
Figure 15: This graph shows the burn-in curves of a single ISFET submerged 3 times in pH 7 solution.	22
Figure 16: This graph shows the burn-in curves of a single ISFET submerged 3 times in pH 10 solution.	22
Figure 17: This graph shows the burn-in curves of a single ISFET submerged 3 times in pH 13 solution.	23
Figure 18 : Burn-in drift voltage using solutions with pH 1 and pH 13	23
Figure 19 : Sensitivity tests (4.01-7-9.21 pH).	24
Figure 20: A fully characterized ISFET wafer.	25
Figure 21: Difference in output voltage between two different measurements under different temperatures in a pH 4 solution (using the same sensor).	26
Figure 22 : Drift voltage (pH 7) for a period of 2 days.	27
Figure 23 : Drift voltage for a period of 2,5 days while using the hotplate with the thermocouple as stabilizer at 25°C.	28
Figure 24: Hysteresis effect for the pattern 7-1-7-13-7. The ISFET is submerged for 30 minutes in each step.	29
Figure 25: The effects that different cell cultures had on the ISFET after being submerged inside for 4 days.	31

Figure 26: Long-term ISFET response inside PBS (pH 7.4)	32
Figure 27 : The gate layers on top of the p-type substrate	33
Figure 28: Overview of the ALD process [10].	36
Figure 29: Overview of the EIS measurement setup	37
Figure 30: CV measurement of the EIS using hafnium oxide as the sensing layer across two pH solutions.	38
Figure 31: Aerosol Jet Printer process schematic.	40
Figure 32: The ISFET after the deposition of the ion-selective membrane using the Aerosol Jet Printer instrument.	40
Figure 33: The sensitivity curves for sodium ions (left) and for potassium ions (right).	41
Figure 34: Top view of the CMi cleanrooms.	46
Figure 35: Project overview in Gantt chart format.	46

List of Tables

Table I: Sensitivity and dielectric constants for different materials as pH sensing layers.	12
Table II: Drift voltage during a 5-minute burn-in.....	20
Table III: Process Flow of the EIS.....	34

1. Introduction

1.1 History and Importance of pH Sensing

When examining the properties of a solution, pH is one of the most important chemical parameters to be aware of. The term was first introduced by Søren Peter Lauritz Sørensen (1868-1939), a Danish biochemist, and is used to denote the acidity or the alkalinity of an aqueous solution [1]. In chemistry, the pH values of a solution are denoted on a scale, usually from 0 to 14. When a solution has a pH of 7 at 25°C, then the solution is called “neutral”. When a solution increasingly approaches pH 1, it becomes more acidic, while when it approaches pH 14 it becomes more basic. This simple way of measuring the acidic and basic properties is incredibly important across many industries as well as ecosystems and organisms, since the value of pH can quickly give an insight into the conditions of an aqueous solution. In agriculture, soil pH is used extensively as a way to monitor soil properties. In environmental studies, the pH of seawater is well studied and continuously monitored. It is an incredibly important parameter to keep track of as the ocean plays a crucial role in carbon cycles. Recent increased carbon dioxide emissions are now changing the pH of the ocean due to ocean acidification [3]. In medicine, the value of pH for living systems across different places of the organism’s body is crucial for health monitoring and treatment. Human blood needs to have a pH of 7.34-7.4 [2]. Deviations from these values can be indicators for illnesses. Of course, knowledge of acidity and alkalinity is also important for safety in handling chemicals, evaluating food products, pool maintenance, water treatment, and much more.

With pH being such a sought-after parameter, a market for pH sensors has naturally followed. Since the invention of the concept of pH by S. P. L. Sørensen in 1920, different types of pH sensors have been invented and sold. More recently, with the introduction of the field effect transistor, different applications of this technology have been used. The ion-selective field-effect transistors (ISFET) was first developed by Piet Bergveld in 1970 and since many different implementations and improvements have been made [5]. These sensors are based on the metal-oxide field-effect transistor (MOSFET) and are called ISFET. This allowed to take advantage of already established production methods and theory, which made it convenient and efficient to reliably produce these sensors. Miniaturization also plays an important role in this push towards using field effect transistors (FET) technology for chemical sensing. However, one of the main drawbacks is that a reference electrode is still required for proper functioning [6].

1.2 Overview of the Internship

Among many companies that produce these sensors, the research and development center “Swiss Center for Electronics and Microtechnology” (CSEM) produces ISFETs within its own cleanroom through a specialized process flow for mass production of ISFETs on 100mm wafers. In this internship, one of the main goals was to examine and characterize the ISFET sensors produced at CSEM from low chemical vapor deposition. In order to achieve this, a packaging methodology must be created for in-house production that is waterproof and

robust against extreme acids and bases, while also being viable for long term usage to enable the characterization. Another aim of this project, was to investigate the possibility of using focused aerosol deposition techniques, to deposit ion-selective membranes for sodium and potassium detection using CSEM's ISFET as the transducer. The final goal of this project was to evaluate hafnium oxide (HfO_2) as a pH sensing layer deposited by atomic layer deposition (ALD), as an alternative to the already standardized deposition process of the tantalum oxide (Ta_2O_5) sensing layer at CSEM. This would be achieved using an electrolyte-insulator-semiconductor device (EIS), constructed at CMi and characterized in NANOLAB. During the internship, an opportunity arose to assess the viability of using the ISFET for pH measurements in cell culture and was incorporated into the project.

Originally, the cooperation between CSEM and EPFL was formed to use the ALD machines at EPFL's cleanrooms (CMi) to deposit both tantalum oxide and hafnium oxide as sensing layers on CSEM's ISFET. Characterization of these ISFET would have then been performed and the results would have been compared. However, the deposition of tantalum oxide using ALD was delayed due to internal organizational issues between the involved parties. Thus, the development of the EIS was introduced as a faster way to perform characterization and evaluation of the differences while these issues were being addressed. Later on, it was reported by the involved parties that ALD of tantalum oxide would not occur during the duration of this internship. The investigation of using ion-selective membranes using focused aerosol deposition on the ISFET were incorporated into the project as a result.

1.3 Description of the Sites

➤ CSEM

CSEM is a research and development center based in Neuchâtel, Switzerland and founded in 1984. The company has a focus in various fields:

- Digital technologies like Internet of Things and smart machinery
- Sustainable energy with a focus on photovoltaics and energy harvesting sensors
- Precision manufacturing

The company's main missions are maintaining the industrial and manufacturing activity inside Switzerland and achieving competitiveness through innovations across its different divisions, which are then passed on to the industrial sector. Its technology transfer process to the industry is one of the more difficult steps of the company. CSEM has deployed several strategies on its approach to combat this issue by diversifying its research across different areas of microtechnology, strengthening the relations between the academia and research and technology organizations within Switzerland, and encouraging start-ups [7].

CSEM has its own cleanroom to enable its focus on precision manufacturing:

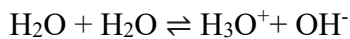
- Built in 2015
- 700m² of cleanroom class from ISO 5 to ISO 7
- Fully automated equipment
- Usage of both 100mm and 150mm wafers
- Industrial production of 150mm wafers

Further information can be found in the Annex.

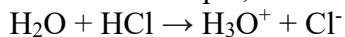
2. The Ion-Sensitive Field-Effect Transistor (ISFET)

2.1 The pH Scale

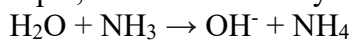
The pH value of a solution is determined by the dissociation of the water inside it. Water in solution tends to ionize:



In order to increase the acidity of the solution, more protons (H^+) must be donated to the solution to increase the H_3O^+ ion concentration and reduce the OH^- ion concentration in the solution. For example, this is achieved by introducing a proton donor in the solution:



While in order to increase the basicity of the solution, an increase of the OH^- ion concentration must be achieved while lowering the H_3O^+ concentration inside the solution. For example, this is achieved by introducing a proton acceptor in the solution:



The amount of hydrogen ions in the solution is thus the marker of the basicity or acidity of the solution. The pH scale is a logarithmic scale that shows the amount of these ions in a solution. The value of pH 7 at 25°C is neutral, while solutions with pH values less than 7 are gradually considered more acidic, while solutions with pH values above 7 are considered more basic. The pH scale thus indicates the amount of hydrogen ion activity in an inverse manner. The larger the concentration of H^+ , the lower the value of pH.

$$\text{pH} = -\log_{10}(a_{\text{H}^+})$$

where a_{H^+} is the activity of the hydrogen ions.

The pH and pOH values when added always add up to 14. For a balanced concentration of $C_{\text{H}^+}=10^{-7} \text{ H}^+$ and $C_{\text{OH}^-}=10^{-7} \text{ OH}^-$, the solution has a pH of 7. If the pH is 4, the pOH is 10 and so on. Lastly, while the typical pH scale has a range of 0 to 14, values lower than 0 and higher than 14 can be achieved [6][19].

2.2 Working Principles

The ISFET (Ion-Sensitive-Field-Effect-Transistor), is a field-effect transistor modified to detect the ion concentration in a solution, such as hydrogen ions, on a pH scale. It was developed by Piet Bergveld in 1970 [5]. The ISFET was introduced as an alternative to the already established glass electrode. Its structure is like that of a MOSFET. However, the difference lies in:

- The gate electrode, which is replaced by the liquid solution which contains the ion concentration for detection and a reference electrode.
- The oxide, where on top of having an insulator protecting the channel (ex. SiO_2), there is also another layer called the “sensing layer” containing the binding sites and is in contact with the solution.

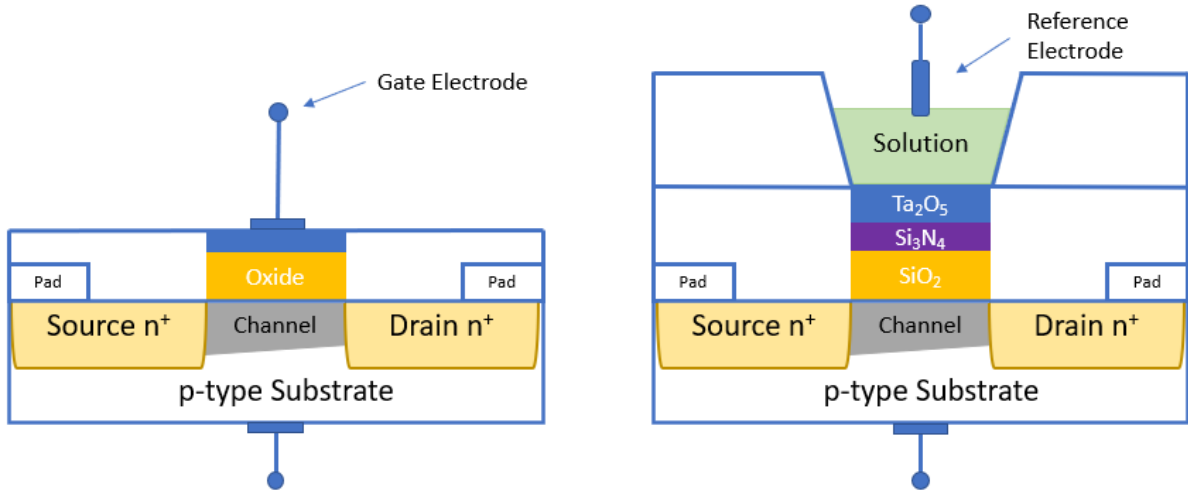


Figure 1 : On the left is a simplified overview of a MOSFET. On the right, a simplified overview of the ISFET produced at CSEM. The gate electrode of the MOSFET is replaced by the solution as well as the reference electrode.

The amount of current that flows through a MOSFET in the linear region of operation is characterized by the equation below:

$$I_{d,lin} = C_{ox}\mu \frac{W}{L} [(V_{gs} - V_t)V_{ds} - \frac{1}{2}V_{ds}^2] \quad (1)$$

where C_{ox} is the oxide capacitance, V_{gs} is the voltage between the gate and the source, V_t is the threshold voltage and V_{ds} is the voltage between the drain and the source.

At this linear operational range, as the value of V_{gs} increases, so does the current flowing through the drain. However, in the case of the ISFET, there is no gate electrode in contact with the oxide of the gate. Instead, the term V_{gs} refers to the voltage between the reference electrode and the source. Ideally, the potential of the reference electrode is the same in all pH solutions. Thus, the current that flows through the ISFET, is regulated by the amount of charge accumulated at the interface between the oxide and the solution, due to an ion sheath.

This interaction between the solution and the oxide is described by the site binding model. The oxides have a certain number of binding sites where the reactions can take place[25]. The charge that is generated on this interface depends on the equilibrium between the Si-OH sites on the surface of the oxide and the amount of H^+ ions available in the solution. In general, the possible amphoteric reactions that take place are listed below:

- -Si-OH (neutral)
- -Si-OH + $H_3O^+ \rightleftharpoons$ -Si-OH₂⁺ + H₂O (acceptor)
- -Si-OH + H₂O \rightleftharpoons -Si-O⁻ + H₃O⁺ (donor)

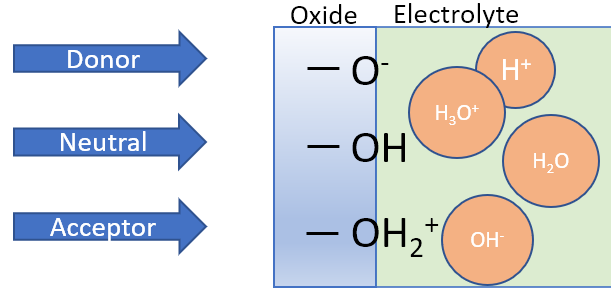


Figure 2: Oxide surface / electrolyte interface. The oxide surface is coated with sites of OH groups that interact with the solution.

One of the most important parameters for a MOSFET is the threshold voltage V_t , which describes the minimum amount of gate-to-source voltage needed to create a conducting path between the source and the drain of the MOSFET. The equation describing this parameter is as follows [6]:

$$V_t = \frac{\Phi_M - \Phi_{Si}}{q} - \frac{Q_{ox} + Q_{ss} + Q_B}{C_{ox}} + 2\phi_f \quad (2)$$

where Φ_M is the work function of the metal, Φ_{Si} is the work function of the silicon. The second term of the equation impacts the V_t due to the accumulated charge in the oxide (Q_{ox}), at the interface between the oxide and the silicon (Q_{ss}) and lastly, the charge in the depletion region in the silicon (Q_B). Q_B is dependent on the doping level of the silicon substrate. In MOSFETs, the threshold voltage V_t is a product of the various processes and parameters it was constructed with. Outside of interferences like radiation, temperature, or degradation of components, the threshold voltage remains the same.

The calculation of the threshold voltage in ISFETs is calculated according to the following equation [6]:

$$V_t = E_{REF} - \Psi + \chi^{sol} - \frac{\Phi_{Si}}{q} - \frac{Q_{ox} + Q_{ss} + Q_B}{C_{ox}} + 2\phi_f \quad (3)$$

where E_{REF} is the constant potential of the reference electrode, Ψ is the interfacial potential between the solution and the oxide and χ^{sol} is the surface dipole potential, which is usually constant. The metal work function has been removed as there is no gate electrode present.

The equation for the interfacial potential Ψ for is the following [6]:

$$\Psi = -2.3 \frac{kT}{q} \frac{\beta}{\beta + 1} (pH_{pzc} - pH) \quad (4)$$

where pH_{pzc} is the value of pH for which the surface of the oxide is electrically neutral. Any change in pH will cause a shift $\Delta\Psi$. This $\Delta\Psi$ is added linearly on the surface potential ϕ_s and thus will cause a shift in the value of the threshold voltage equal to $\Delta\Psi$ [6].

$$V_t = \Delta\Psi = -2.3 \frac{kT}{q} a \Delta pH \quad (5)$$

where a is a dimensionless parameter that ranges between 0 and 1 and is dependent on the surface properties of the sensing layer. The maximum potential per unit pH is limited by the

Nernst equation to be $\sim 59.2\text{mV}$ per pH unit at 27°C . Thus, the maximum $\Delta\Psi$ per pH unit is limited. In fact, if $a=1$, the sensing layer provides the maximum possible sensitivity [6].

Much research has been dedicated to finding the best sensing layer for ion detection. Different layers provide different values for a as shown in Table I. High- k dielectrics such as tantalum oxide and hafnium oxide have shown to have excellent sensing capabilities [19][13][18][17][21][23]:

Sensing Layer	Dielectric Constant	Sensitivity (mV/pH)
SiO_2	3.9	$\sim 20\text{-}35$
Si_3N_4	7	$\sim 53\text{-}55$
Al_2O_3	9	$\sim 54\text{-}56$
Ta_2O_5	22	$\sim 56\text{-}59$
HfO_2	25	$\sim 58\text{-}59$

Table I: Sensitivity and dielectric constants for different materials as pH sensing layers.

In the case of the ISFET, the threshold voltage of the ISFET changes with the number of charges present at the sensing layer which depends on the pH as well as the properties of the sensing layer. Different pH solutions would produce different amounts of charges at the surface, consequentially changing the drain current according to equation (1). This is the fundamental principle for sensing using FET technology.

2.3 The Reference Electrode

The Reference electrode varies from implementation to implementation. For the ISFET explored in this report, a double junction Ag/AgCl glass electrode was used and is visible in Figure 3. The electrode, once submerged into a solution, provides a stable reference potential.



Figure 3 : The double junction reference electrode reference electrode.

The inside of the glass electrode contains a silver contact where a probe can be connected to. On the other end, it interfaces with a silver chloride wire which is submerged inside a 3M KCl solution (potassium and chloride are used together because of similar mobility constants). This solution then interfaces with the pH solution through a frit (a porous junction). The height of the solution inside the reference electrode must always be higher than the height of submersion of the reference electrode inside the solution such that the potassium chloride solution inside the solution does not get contaminated with the contents of the solution. However, some potassium chloride escapes into the pH solution but since the amount is so low it can be negated in the case of pH sensing. The valve at the top needs to be open when it is submerged into the solution and closed during storage.

To verify the functionality, another reference electrode can be used. Both are submerged inside the same solution and the difference in voltage between the two reference electrodes is checked using a simple multimeter. If the absolute value of the voltage output is around 10-20mV both electrodes can be classified as operational. Bigger values than this is an indication that one or both of the reference electrodes are faulty.

2.4 ISFET Development Process at CSEM

CSEM has its own industrial process and its own clean room for developing ISFETs.

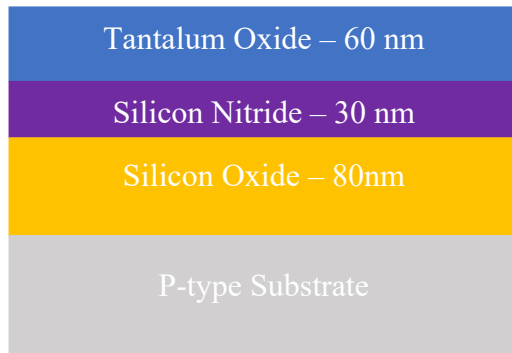


Figure 4: Gate stack layers produced by CSEM. The thicknesses might vary slightly from chip to chip.

The process involves 67 steps in total. One of the critical steps is the formation of the gate stack layers. The stack interfacing with the substrate is made up of silicon oxide (SiO_2) grown by the process of dry oxidation. The sensing layer chosen, the layer that interfaces with the solution, is Ta_2O_5 deposited by LPCVD. Between the silicon oxide and tantalum oxide layer rests a 30nm thick silicon nitride protective interlayer. The reason for the existence of this layer was reported from personnel who worked on the original process flow: After the required crystallization of the tantalum oxide, it was reported that the material

diffused into the silicon oxide. This intermediate layer was successful in stopping this diffusion from taking place, and thus was integrated into the process flow. Through further investigation, they discovered that the tantalum oxide was prone to chemical attacks, which carved a path through the tantalum oxide and onto the silicon oxide. The silicon nitride interlayer stopped the chemical attacks from reaching the silicon oxide and damaging the sensor further. CSEM's ISFETs are also protected by a platinum shield, with only the gate being exposed along with the pads for the source and drain contacts. The fabrication also creates a diode-based temperature sensor on the same chip giving the option to have an on-chip temperature sensor that is located very close to the gate. This process yields 218 ISFET chips as shown in Figure 5.

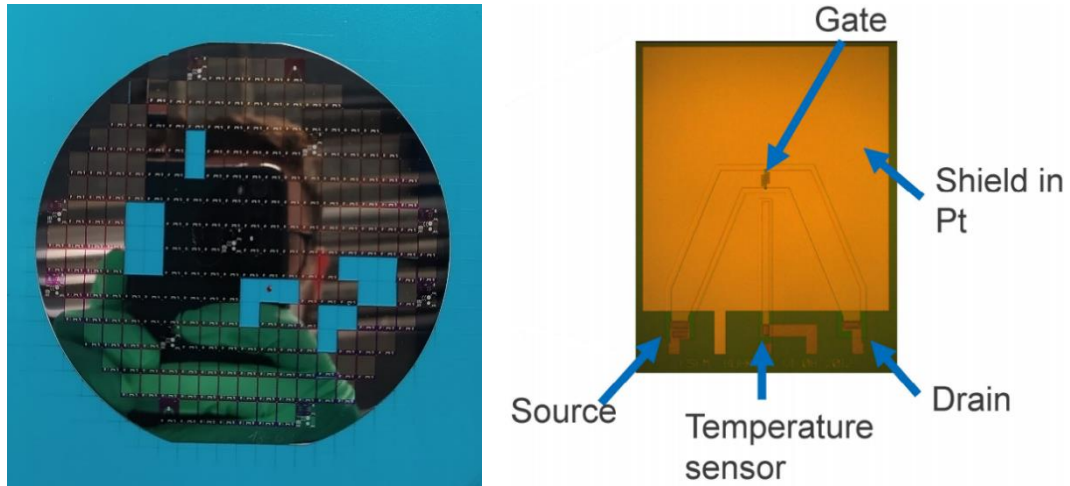


Figure 5 : A diced 100mm wafer for the fabrication of 218 ISFET chips (left). On the right is an image of a single ISFET. Both Source and Drain contacts are visible, and there are also 2 more contacts for a diode that can be used as a temperature sensor.

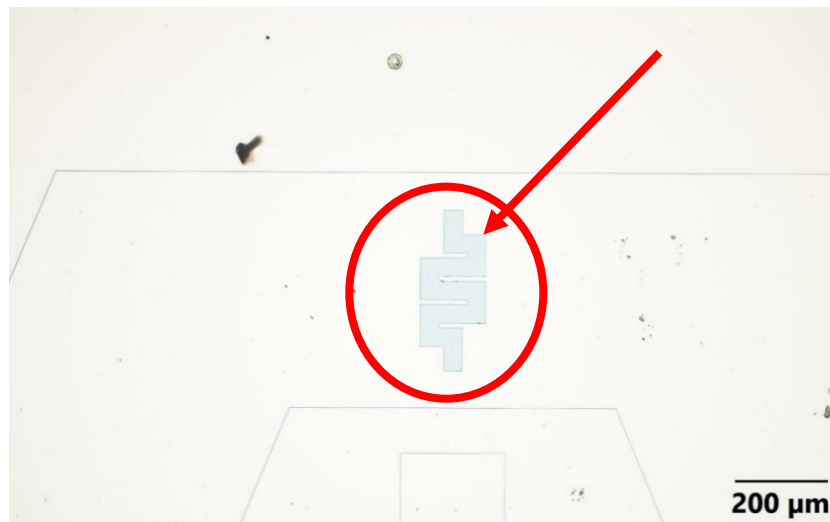


Figure 6 : A closeup of the gate under an optical Microscope. The encircled geometry must always be exposed to be in contact with the solution.

3. Packaging

3.1 Criteria and Challenges

The PCB that was selected for this project had to be slim, while also being long enough and so that the ISFET can be submerged into solutions deep enough while still protecting the exposed circuitry at the other end. Figure 10 displays the PCB that was used for the packaging of all ISFETs in this project.

The most challenging aspect for creating the packaging was the creation and application of the epoxy. In short, the epoxy had to be resistant to an array of different acidic and basic solutions, from pH 1 to 13. At the same time, it should also protect the wire bonds, the pads and the PCB wiring from coming into any contact with the solution, as this would cause leakage current and would make the measurements unreliable. Lastly, the epoxy should have as little trapped air bubbles as possible inside it. Failure to do so could cause material breakdown over time and oxidation of the wires if any trapped gas was in contact with a wire.

3.2 Preparation of the Epoxy

In order to improve adhesion, the PCB's must be properly cleaned first. In order to do so, they are submerged into a container of acetone, which is then placed inside an ultrasonic bath machine called "BANDELIN Sonorex Digiplus", in order to clean the substrate of any chemical contaminations or other particles.

For the PCB to work correctly and avoid leakage current, special care must be taken when applying and making the epoxy. The main issue that occurred was unwanted air bubbles inside the epoxy on the PCB, even after the epoxy was cured. The epoxy glue was prepared with the following components and ratios:

- 2-parts Araldite AY 105-1 as the base component
- 1-part Harter HY 991 as the curing agent.

Many different methods were tested for the degassing of the epoxy, including using hot water baths for both of the components before and after mixing, plasma treatment, as well as vacuum. However, due to the high viscosity and its short application lifetime such methods were ineffective.

Fortunately, a planetary mixer "Thinky Mixer" was made available to successfully mix the epoxy components. It uses both planetary and rotational motion to both mix and degas the components. Set at 2000 revolutions per minute for four minutes, it was sufficient to mix the components all while not introducing new air bubbles. This proved to be the fastest and most effective way of degassing. Every PCB that was since produced, included epoxy mixed and degassed with this method. The only difference observed was that the optical properties of the mixture had changed (Figure 7). However, this did not induce any

noticeable differences in the robustness of the epoxy. Finally, in order to cure the epoxy, the PCBs are placed inside a pre-heated oven at 100 °C for 10 minutes.

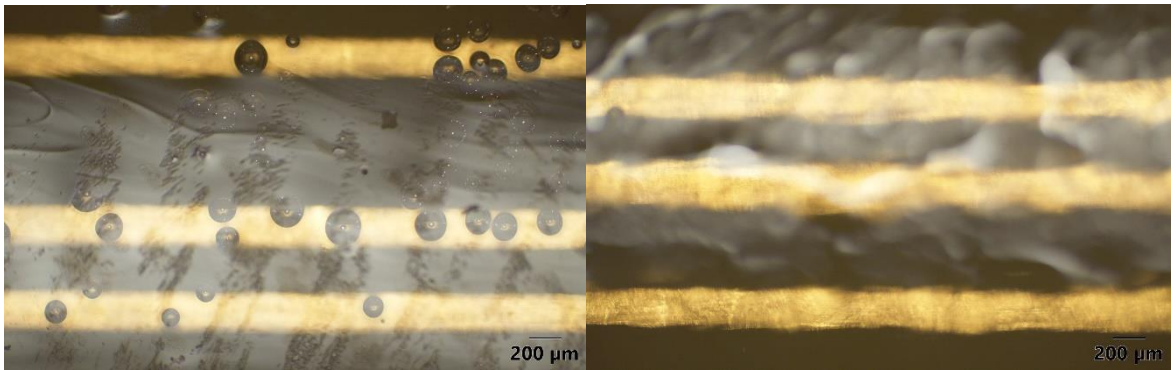


Figure 7 : Epoxy on the PCB without using Thinky Mixer (left). Epoxy on another PCB with 4 continuous minutes of mixing with the Thinky Mixer (right).

3.3 Wire Bonding

To perform the wire bonding, a “TPT wire bonding” machine was used, in manual mode. The wire bonding machine uses an ultrasonic power and force to stick the wire onto the PCB and the contacts on the ISFET. The correct values for this procedure, the power of the pulse, the Force and time of contact, were obtained through trial and error, such that the bondage points do not obstruct the current passing through, while still being bonded strongly enough that the wire does not detach due to small vibrations.



Figure 8 : Wire bonder machine (left), The wire bonded ISFET chip (right).

For this machine, the following values were used:

For the first Bond:

- US P(mW) = 350
- Time(ms) = 300
- Force (mN) = 286

For the second Bond:

- US P(mW) = 340
- Time(ms) = 300
- Force (mN) = 300

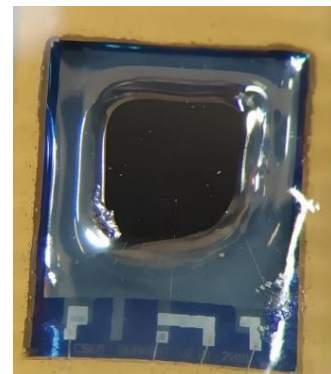


Figure 9: A closeup of the encapsulated sensor. The gate in the middle is clearly exposed.

3.4 Fine Encapsulation

One of the more critical aspects of the encapsulation was the application of the epoxy around the gate and the wire bonds. This proved to be most time-consuming step of the entire process, as the epoxy dispensing needed to be incredibly accurate to not break the wire bonds or cover the gate. To overcome these issues a different epoxy was applied, which was more resistant than the previous epoxy while being more viscous. The epoxy was made of the following list of components:

- 1-part Aerosil 200 as a viscosity modifier
- 5-parts Jeffamine D230 as the curing agent
- 15-parts EPON Resin 825 as the base component

Once again, the new epoxy had to be degassed. The planetary centrifugal mixer was used with the following recipe:

1. 3 minutes of mixing at 2000rpm
2. 15 minutes of degassing at 2200rpm
3. At least 15 minutes break to avoid damage to the machine from overheating
4. 3 minutes of mixing at 2000rpm
5. 15 minutes of degassing at 2200rpm
6. 3 minutes of mixing at 2000rpm

Mixing was performed between each degassing step as to not risk separation of the components.

A pneumatic dispenser from the company “METCAL” was used that can accurately dispense the epoxy. Exceptional care was taken such that during the epoxy dispensing the epoxy would not spill over and cover the gate. The AEROSIL 200 was used to increase the viscosity so that accurate dispensing could be performed. Some air bubbles were still introduced during the transfer from the planetary centrifugal mixer container to the syringe used by the pneumatic dispenser and during the application of the epoxy, mainly under the wire bonds.

After the epoxy dispensing is complete, it is left overnight in a protected area at room temperature as curing the epoxy in the oven immediately after its application would lower its viscosity again and spill over the gate. The increased viscosity from the AEROSIL 200 viscosity modifier made sure that during this curing time, the epoxy is stable and does not spill over the gate. On the following day, curing takes place inside a pre-heated oven at 80°C for 4 hours.

3.5 Main Body Encapsulation

Once the final encapsulation of the ISFET surface is complete, the epoxy is applied on the front face of the PCB where the wiring is visible and then placed into the oven at 100°C for 10 minutes once again. Some air bubbles were trapped between the interface of the epoxy and the PCB. However, these air bubble defects pose no issues to the stability of the packaging since no contact with the wires is made and are of qualitatively very small size. In total, over 70 ISFETs were packaged with this methodology, which demonstrates the reproducibility and reliability of this packaging methodology. With the packaging now complete, the sensors are tested and characterized.

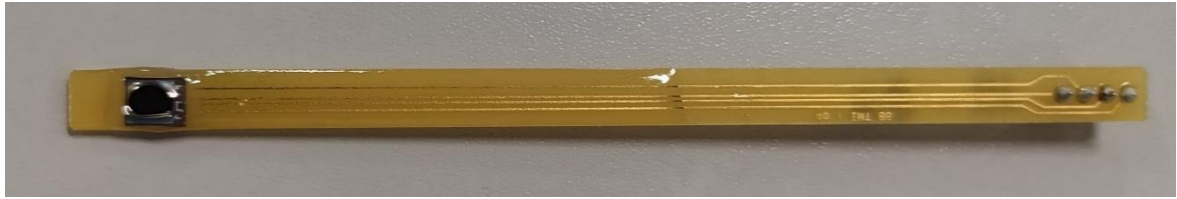


Figure 10: Image of an encapsulated ISFET.

4. Characterization of the ISFET

4.1 Measurement Setup

The ISFETs were measured in two different setups. A probe station using a semiconductor parameter analyzer “Hewlett Packard 4155A” and a setup for continuous and long-term measurements shown in the figure below.

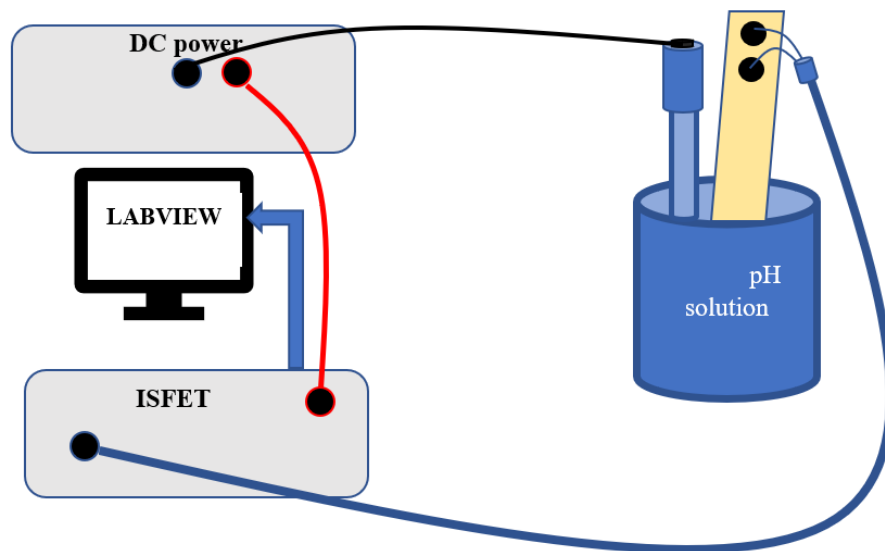


Figure 11 : The overview of the ISFET measurement setup. The reference electrode submerged in the pH solution generates a stable voltage. The ISFET amplifier maintains the drain current at $100\mu A$. The voltage required to maintain that constant drain current value is read by the computer through a GPIB connector and constitutes the output signal of the ISFET.



Figure 12 : ISFET amplifier. On the top right screen, the amount of leakage current detected from all the active ISFETs. On the display below, the output voltage is displayed depending on which channel is selected.

A program created with LabView collects these data points from the GPIB output of the ISFET amplifier. Depending on the sampling rate, it produces an average of multiple data points as an output. These outputs are recorded in a .txt file along with respective date and time of measurement.

4.2 Burn-in Response and Reproducibility

ISFET burn-in refers to the behavior of the response of the sensor from submersion until equilibrium is reached in the solution. The first burn-in test was performed to assess the functionality of the sensor. During this period, early failures occur, such as presence of leakage current or general non-functionality. These issues could occur due to faulty packaging allowing the solution to move under the epoxy and make contact with the PCB wiring or due to the ISFET itself having been damaged in fabrication or later during the packaging procedures. The latter is sent for repackaging and the former is discarded.

The ISFETs were tested in pH solutions of 1-4-7-10-13 at 25°C and burn-in curves were recorded. In this instance, burn-in was estimated for five minutes across each pH solution. This test allows to assess the response of the sensor when it comes into first contact with a solution.

pH value	Contents	Time	Drift Voltage
1	Glycine / hydrochloric acid	5 minutes	~18mV
4	Citrate / hydrochloric Acid	5 minutes	~25mV
7	Phosphates	5 minutes	~30mV
10	Boric acid / potassium chloride / sodium hydroxide	5 minutes	~60mV
13	Potassium chloride / sodium hydroxide	5 minutes	~12mV

Table II: Drift voltage during a 5-minute burn-in

Drift was observed across all pH solutions. However, the amount of voltage drift varied significantly across each pH solution. In general, the pH extremes of 1 and 13 tended to stabilize much faster than the rest. By far, pH 10 was the slowest to detect, with a drift of 60mV, equal to an entire pH unit. The drift was very reproducible across multiple tests and tended to stabilize after 30 minutes of continuous submersion. In general, multiple tests in the same pH solution tended to converge after 5 minutes, even with their small initial variations. However, since this drift is predictable, further adjustments can be made through post-processing of the signal to improve the accuracy by prediction. By observing the initial response output of the ISFET, conclusions can be drawn on the point of stabilization that will be reached with high accuracy, which can prove useful if the sensor is required to perform quick measurements. Nevertheless, it is advisable to further research methods to increase the burn-in time or reduce the amount of burn-in voltage drift.

One point of note is the reproducibility of the burn-in curves across different sensors. Multiple ISFETs went through the burn-in tests, however, it was observed that the drift voltage in each pH solution had slight variations. This would mean that in cases where software is performing post-processing of the output signal of the sensor to speed up the results, an evaluation for the burn-in curves of each ISFET separately would be of interest.

The working point is a reference to the value of the output voltage a sensor produces after being submerged into a solution of pH 7 for an adequate time until the stabilization of the output. The ISFET working point is another important characteristic that is discovered through the burn-in tests. ISFETS originating from the same wafer showed to have different working points at pH 7 with a deviation up to 1V. An investigation took place to evaluate the possibility of a correlation between the position of the ISFET on its wafer and this deviation in the working point. However, no correlation was found. An ISFET could have a working

point that differed up to 1V from a neighboring ISFET on the wafer. Such a behavior could occur due to the introduction of impurities in the gate stacks among one of the steps in the process flow or due to uneven implantation/deposition.

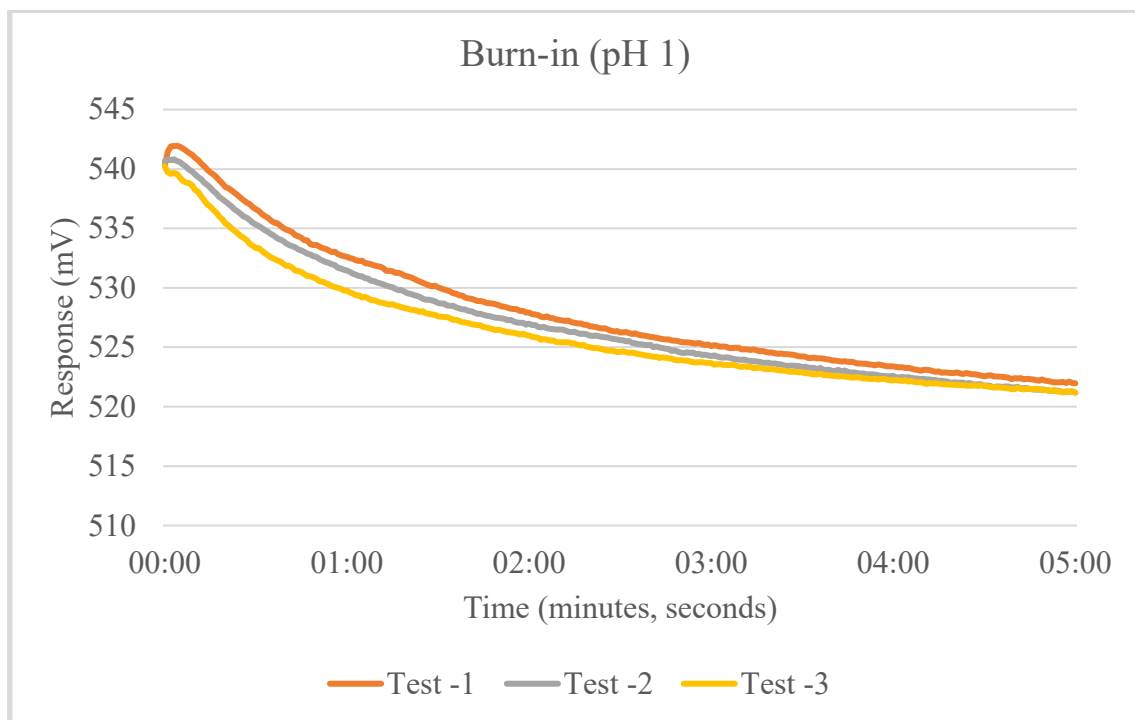


Figure 13: This graph shows the burn-in curves of a single ISFET submerged 3 times in pH 1 solution

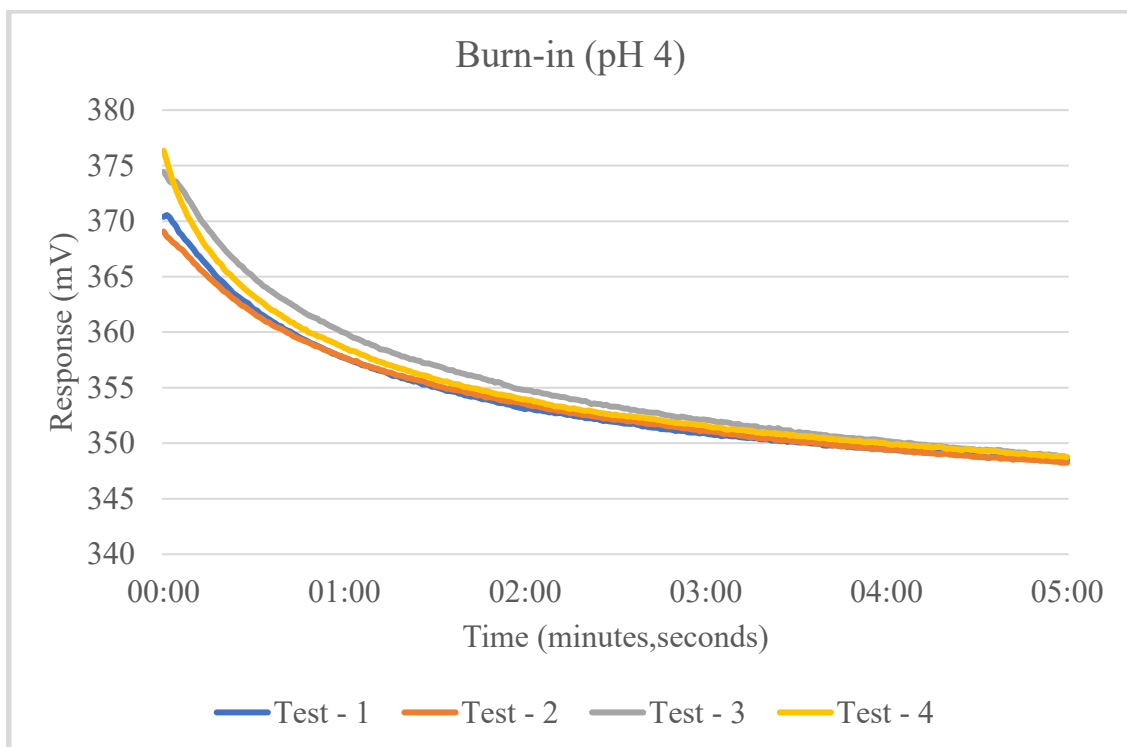


Figure 14: This graph shows the burn-in curves of a single ISFET submerged 3 times in pH 4 solution.

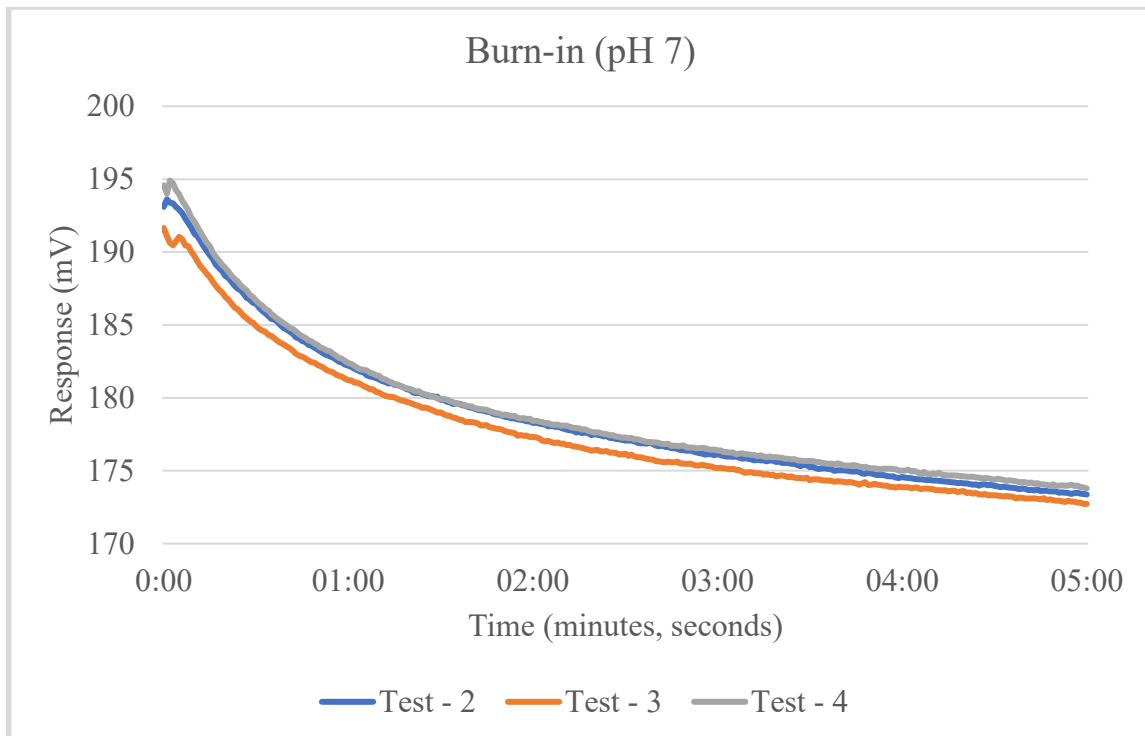


Figure 15: This graph shows the burn-in curves of a single ISFET submerged 3 times in pH 7 solution.

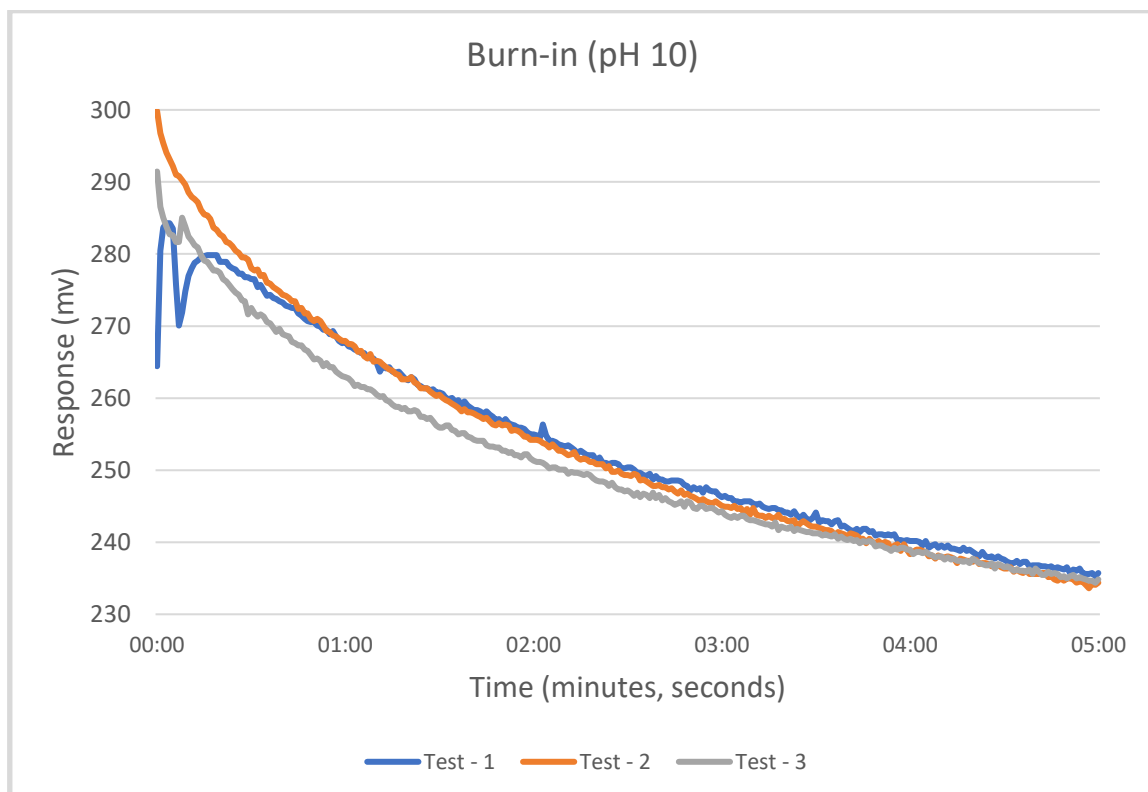


Figure 16: This graph shows the burn-in curves of a single ISFET submerged 3 times in pH 10 solution.

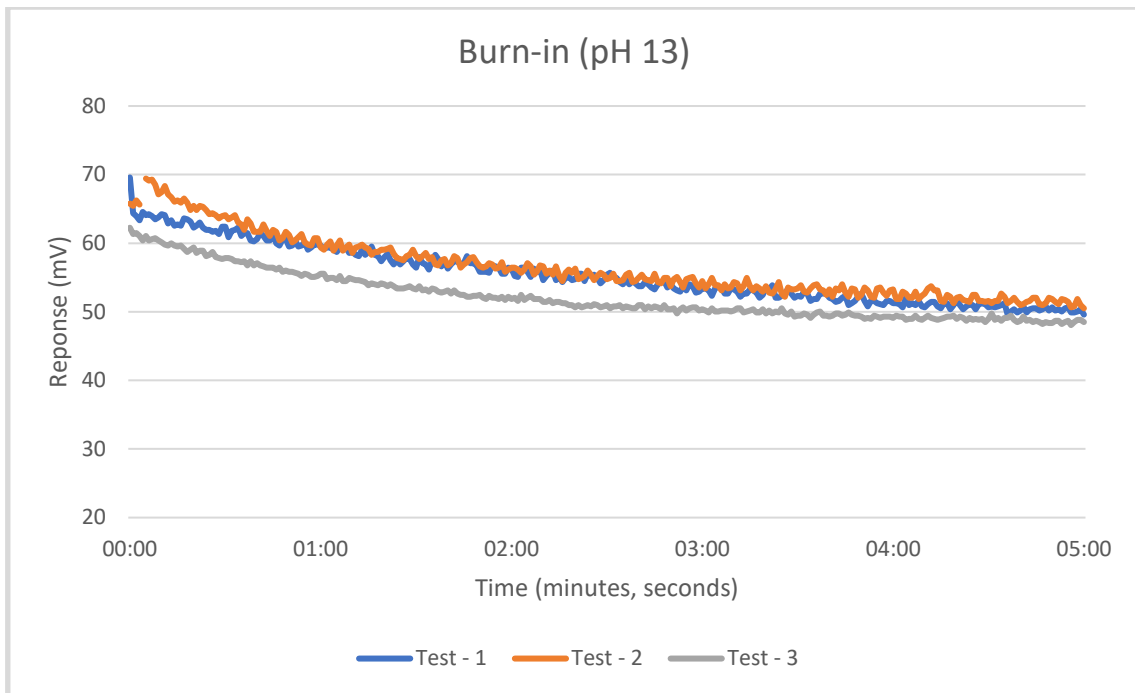


Figure 17: This graph shows the burn-in curves of a single ISFET submerged 3 times in pH 13 solution

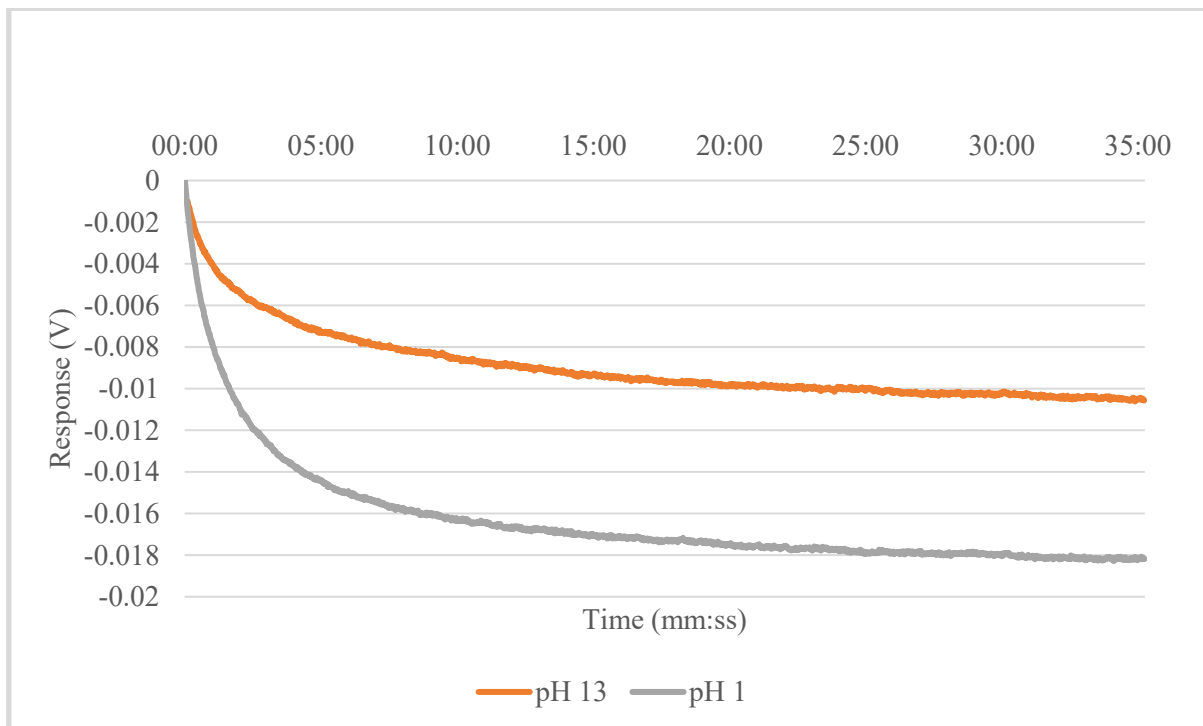


Figure 18 : Burn-in drift voltage using solutions with pH 1 and pH 13

4.3 Measuring Sensitivity

Once the ISFET is assessed as functional through the burn-in test, the sensitivity can be tested using different pH solutions (Figure 19).

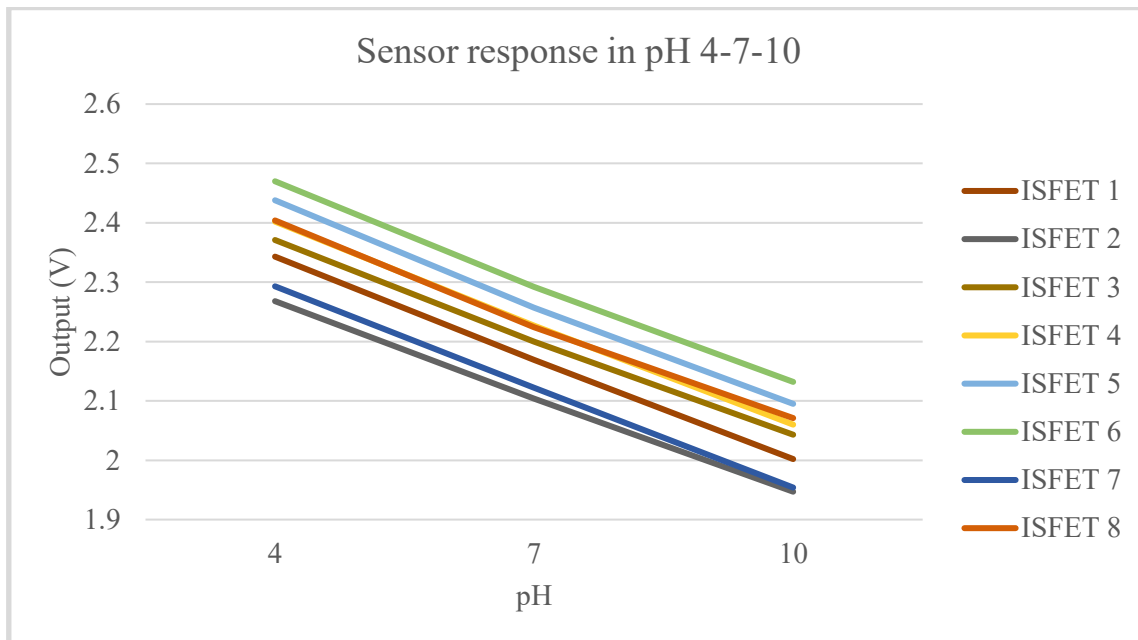


Figure 19 : Sensitivity tests (4.01-7-9.21 pH) each line represents a different ISFET. All chips showed good sensitivity responses with around 58 mV per unit pH, close to the Nernstian limit for the Nernst Equation predictions for hydrogen. There is also again a high variation between the working points of each ISFET.

One of the main concerns when extracting the corresponding voltage of an ISFET inside a solution with a certain pH, is the time needed for the stabilization. As an example, two solutions containing pH 1 and pH 13 were measured over the course of 35 minutes. The results are shown in Figure 18. The output voltages are changing over the course of time, while all the bonding sites on the surface are slowly being occupied and equilibrium is established in the solution.

In order to quickly evaluate such a large number of sensors while taking into account the errors due to burn-in, a quick evaluation test was created where each ISFET output is recorded and checked based on its sensitivity and R-squared values in pH 4, 7, and 10. If the sensitivity falls outside of the range of 52-62mV/pH or the R-squared value is not within the acceptable range value of $r^2 > 0.95$, then the ISFET fails and will not be packaged. Figure 20 shows the results of the application of the quick evaluation.

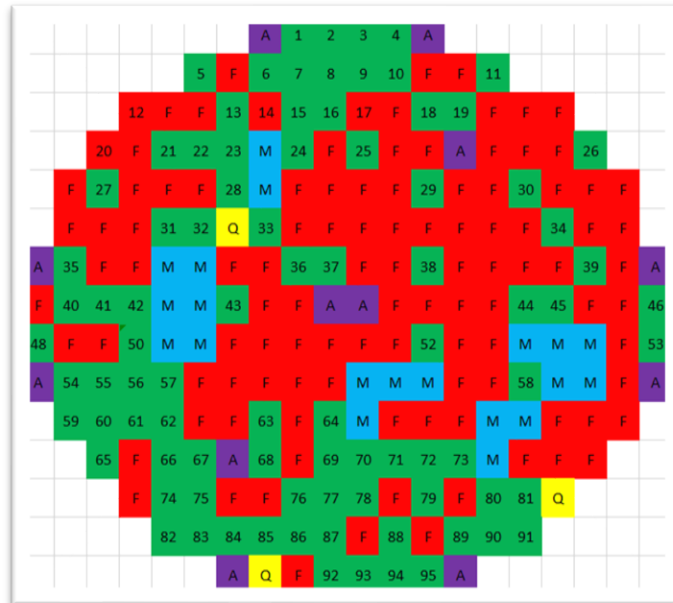


Figure 20: A fully characterized ISFET wafer. The chips with red color have either failed to pass the quick evaluation test or have had issues during production in the cleanroom, while chips with a green color have passed the tests. In this case, there was an issue with the lift off process that left the gate of the sensor covered. Sites with the letter « A » mean that the chip was used for alignment and/or testing. Sites with the letter « M » signify that the chip has been removed before exiting the cleanroom.

In general, the sensors were found to have near Nernstian response close to $\sim 58\text{mV}$ per pH unit and showed high linearity despite the speed of the measurements.

4.4 Temperature Dependence

Temperature is a crucial factor to be considered in order to perform precise measurements. Like the MOSFET, the ISFET is also prone to temperature influences that will change the threshold voltage and lead to inaccurate measurements or leakage current. This is dependent on the pH of the solution [27], the parameters of the semiconductor as well[15]. Using the same setup, the response of the ISFET for temperatures of 25°C , 35°C , and 45°C are measured for different pH solutions.

Different pH levels showed different output voltages for the same temperature. Solutions containing pH of 1, 7, and 13 were compared in temperatures of 25°C , 35°C , and 45°C . Overall, the divergence due to temperature was increasing with increasing acidity. Another factor to consider is the temperature of the reference electrode as it will influence the measurements. In order to avoid any offsets in the output, contact with the solution and the reference electrode was minimized. The fluctuation of potential of the reference electrode due to change in room temperature was not taken into account. The measurements overall produced:

- $\sim 3.0\text{mV}/^\circ\text{C}$ for pH 4
- $\sim 2.6\text{mV}/^\circ\text{C}$ for pH 7
- $\sim 2.2\text{mV}/^\circ\text{C}$ for pH 10

As mentioned in section 4.3, the sensitivity of the ISFETs developed at CSEM is $\sim 58\text{mV}$ per pH unit. This helps to illustrate how important the role of temperature plays when extracting the correct pH value of a solution. A 10°C difference in the solution would introduce half a unit of pH as error. The ISFETs characterized using the ISFET amplifier were very sensitive to temperatures, which meant that for lab temperatures a thermal stabilizer was required for precise measurements.

4.5 The Isothermal Point

An important parameter when studying how temperature affects the ISFETs is the isothermal point. The isothermal point is a certain value of the drain current I_D , under which the temperature variation of the chip has as little as possible an effect on the output. This value will be represented by I_{IS} . Each point in the pH scale has its own isothermal point (I_{IS}), and individually each ISFET isothermal point will be slightly different due to variances introduced by the cleanroom processes. By biasing the ISFET to operate at I_{IS} , minimization of the effects of temperature can be achieved, providing a more stable sensor.

The ISFET amplifier available in this project is set to bias the ISFETs under drain current $I_{OP}=100\mu\text{A}$. This value was chosen in the past when constructing the ISFET amplifier, as it was measured to be the $I_{IS,\text{pH } 4}$ which is the isothermal point of pH 4, meaning that when characterizing an ISFET inside a solution of pH 4, changes in temperature would have a less pronounced effect on the output signal compared to any other pH point. However, as explained in the section 4.4, the ISFET turned out to be very sensitive to temperature fluctuations. This did not align with past experiments. Investigations were performed under the semiconductor parameter analyzer that showed that the isothermal point for pH 4 to be around $I_{IS,\text{pH } 4}=180\mu\text{A}$. This is a large deviation from the past and is a result from recent changes in the cleanroom equipment and processes. It is therefore advised to either change drain current used for operating the ISFETs (I_{OP}) or modify the process flow parameters of the cleanroom. In Figure 21, the difference between the output voltage of the sensor between submersion in solutions with different temperatures is recorded on the y axis, while the drain current is displayed on the x axis. The graph shows that the point where the difference in the outputs is 0 is at $\sim 180\mu\text{A}$, while past that point, the difference becomes negative.

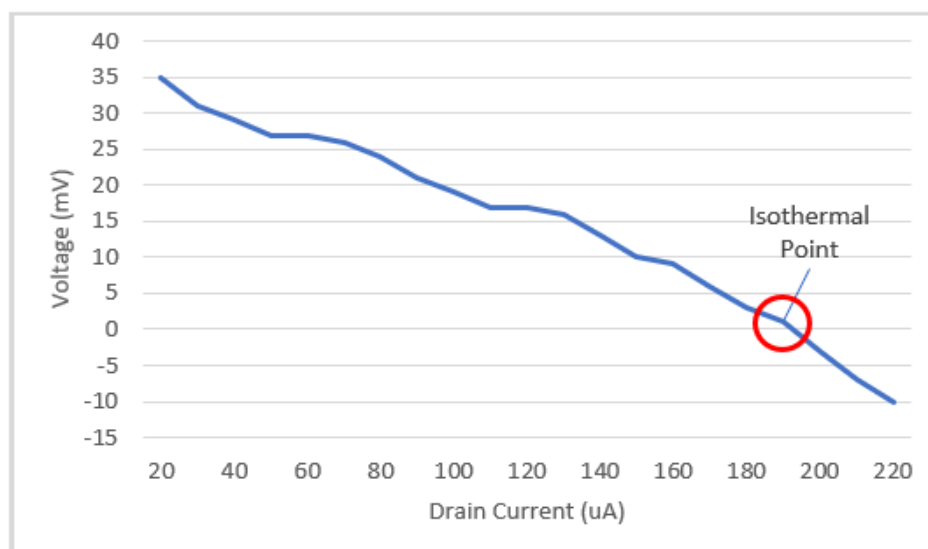


Figure 21: Difference in output voltage between two different measurements under different temperatures in a pH 4 solution (using the same sensor).

4.6 Long-Term Voltage Drift

Long term drift refers to the voltage drift that will occur when the sensor is in operation inside a solution for multiple hours or days. Unlike burn-in, long term voltage drift is the drift that is recorded after the sensor has stabilized. Such properties are of interest, as the sensor can be left inside a solution for days, providing constant feedback. To evaluate the long-term drift, the sensors were left inside a pH 7 solution for over the course of 2,5-3 days.

Initially, the effects of temperature were not considered, which caused major variation in the output voltage, visible in the Figure 22. During the daytime, when temperature rises, the temperature of the lab follows, which increases the output voltage around 5-6 mV which is expected after studying the temperature dependence. To control for temperature, a hot plate with a thermocouple was used to keep the temperature as stable as possible at 25°C. The results are visible in Figure 23.

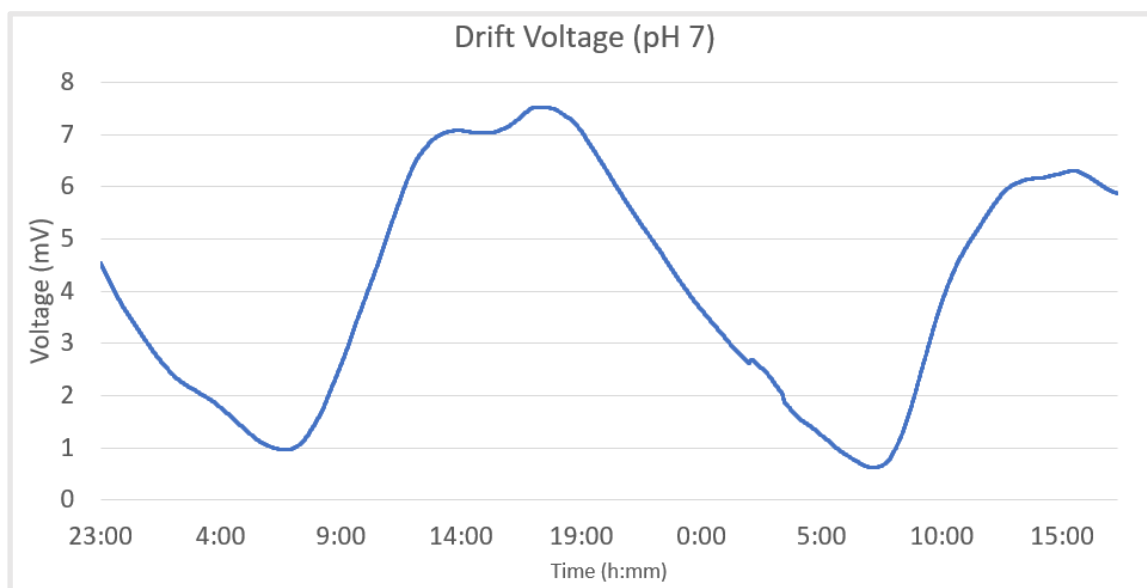


Figure 22 : Drift voltage (pH 7) for a period of 2 days. By observing the time of day in the x axis, in the evening the voltage drops while it rises during the day as the lab temperature fluctuates.

However, even with a thermocouple, the results were still not perfectly stable. In the case of pH 7, the deviations ranged around 0.5mV which while low show that there is a limit to accuracy. The response in pH 4 was slightly more volatile, which could be attributed to larger fluctuations of temperature during these days or due to pH 4 being slightly more sensitive to temperature than pH 7. However, by observing the long-term drift, its value of the voltage drift is less than 1mV, showing that the ISFET is indeed capable of long-term measurements if control of the temperature can be achieved. The effects of temperature on the sensor can also be reduced by changing the I_{OP} of the ISFET. Operating with drain current closer to the Isothermal point should improve the stability of the long-term measurements even further.

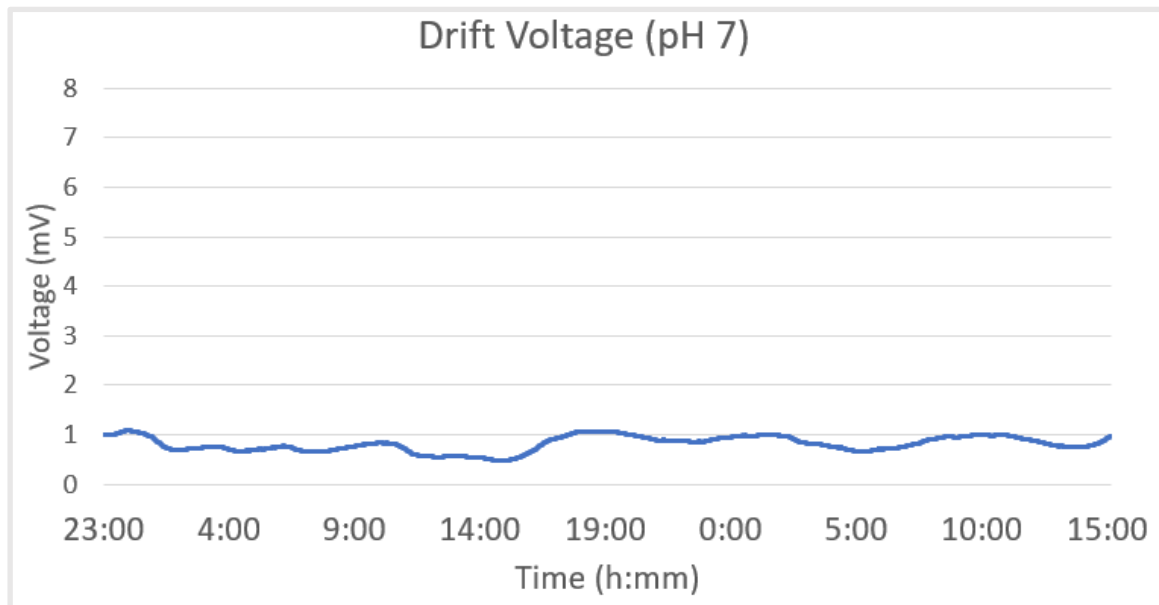


Figure 23 : Drift voltage for a period of 2,5 days while using the hotplate with the thermocouple as stabilizer at 25°C. This time the variation is much lower at a value around ~ 0.5mV.

4.7 Hysteresis

Hysteresis, in the case of the ISFET, is characterized as the lasting effect a measurement with a certain pH may have on the sensor, as to influence the result of the subsequent measurements inside solutions with different pH. Here, this effect is observed by first stabilizing the sensor response inside a solution of pH 7. Afterwards, the sensor is submerged in the following succession of pH solutions: 7→1→7→13→7. The effects of hysteresis were observable by comparing the response of the sensor in pH 7, before and after it was submerged in a solution of pH 1 or pH 13.

The same sequence was examined twice for different submersion times.

- **Response in pH 7:** 62mV→61,38mV→62,6mV, loop time: Submersion time = 10 minutes
- **Response in pH 7:** 78mV→79,2mV→78,9mV, loop time: Submersion time = 30 minutes

The results show that the hysteresis effect is larger when the ISFET was submerged for a longer period with a maximum of 1,2mV of deviation. With a submersion period of 10 minutes, the deviation of 0,62mV. This shows that when performing hysteresis tests, a longer time of submersion leads to higher deviations in the response. This effect must be considered when performing precise measurements, as 1.2mV of error translates to an error of ~0.2pH.

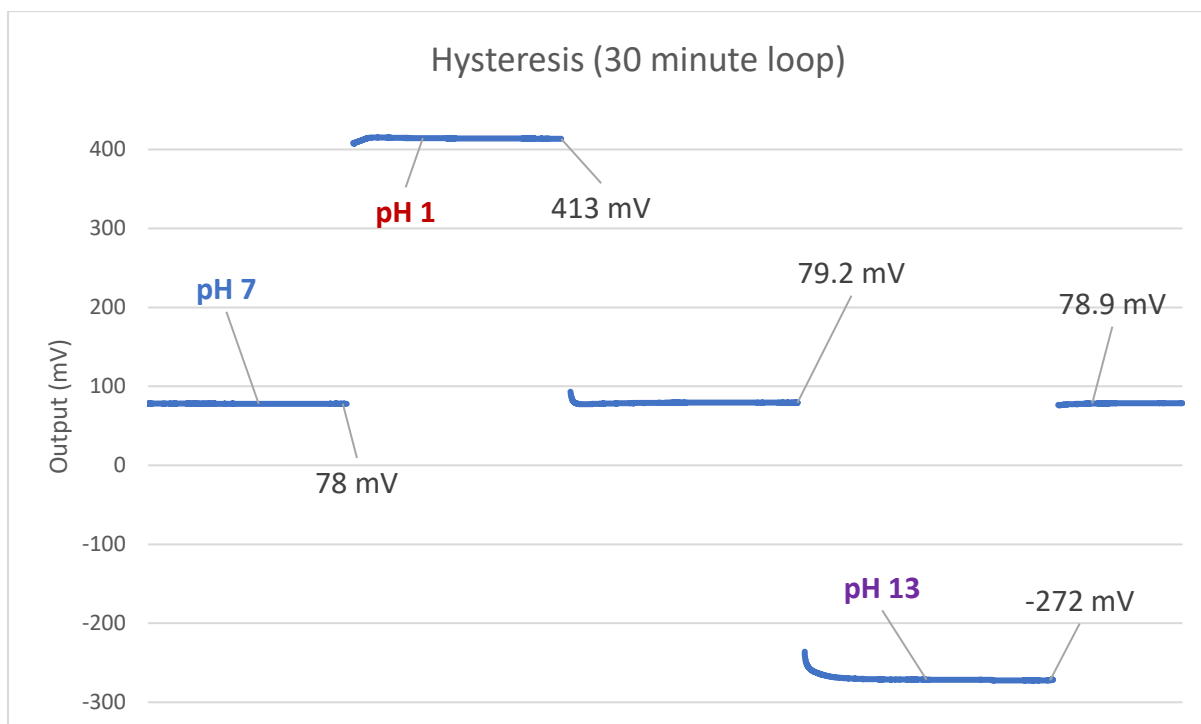


Figure 24: Hysteresis effect for the pattern 7-1-7-13-7. The ISFET is submerged for 30 minutes in each step.

5. Testing ISFETs for Biological Applications

5.1 Overview

ISFETs are met with great interest for applications in the field of biology. As described before, the importance of pH of a solution is of significant importance, especially when there are microorganisms involved. Parameters such as nutrient concentration and maintaining the correct environment for cell growth inside the laboratory are controlled by the pH of the cell culture. There is interest internally and externally of CSEM for these kinds of sensors that can provide accurate pH measurements. Another usage for ISFETs would be to provide long-term continuous measurement of the cell culture. As discussed in section 4.6, CSEM ISFETs can make multiple day measurements with minimal drift. This could potentially prove that the ISFET is a suitable candidate for cell culture monitoring. Due to its small size and robustness, this ISFET can also be placed inside incubators for extended periods of time.

5.2 Bio-Compatibility of the ISFET

Before any measurements can be executed, there needs to be an evaluation of the compatibility of the packaged ISFET, the epoxies used for packaging, and the PCB. A sensor intended for these kinds of uses needs to be first sterilized so that no bacteria or spores will contaminate the cell culture it is supposed to measure. There were two available methods that were considered for sterilizing the packaged sensor, “ethylene oxide sterilization” (EOT) and “X-ray sterilization”.

Ethylene oxide (C_2H_4O) is an alkylating agent that is used to stop the reproduction of microorganisms across the device. The ethylene oxide sterilization process is compatible with equipment that has already been assembled, does not use high heat or radiation, and is ideal for sterilizing an ISFET.

X-ray sterilization was also considered; however, it has been reported that the radiation emitted by the equipment would influence the electrical characteristics of a MOSFET [22]. Since the ISFET shares similar working principles, this was not chosen as a viable sterilization method. Characterization of the sensors was performed before and after the ethylene oxide sterilization process. No noticeable effects were observed before and after the process. This shows that EOT is a viable sterilization process for CSEM ISFETs which is highly valuable, as the sensors would need to be sterilized frequently for usage. The ISFETs were submerged inside different cell culture solutions shown in Figure 25:

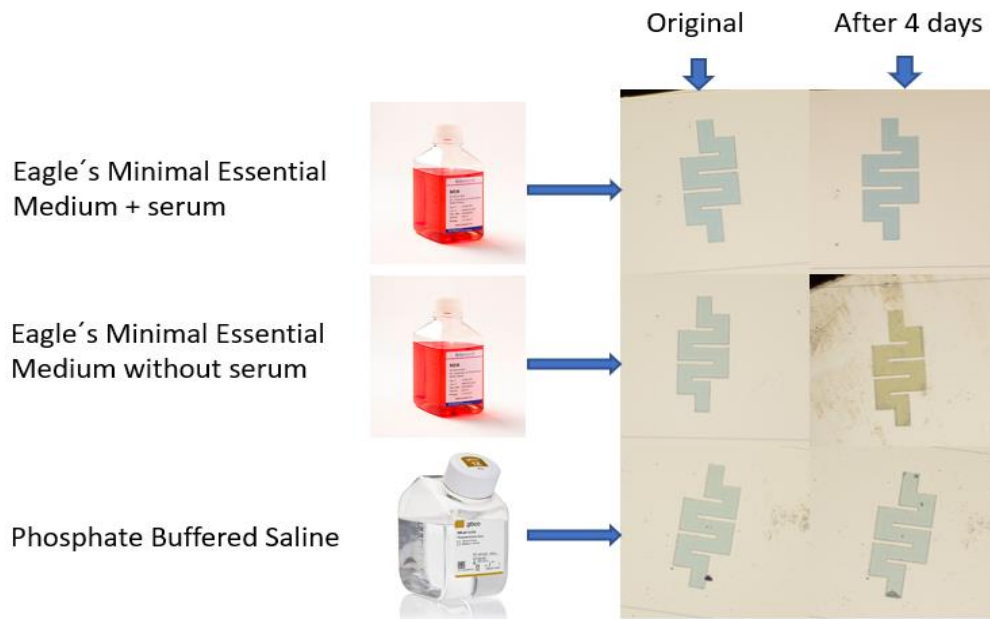


Figure 25: The effects that different cell cultures had on the ISFET after being submerged inside for 4 days.

Phosphate buffered saline with pH of 7.4 (PBS) had no optical effect on the ISFET. Eagle's Minimal Essential Medium (EMEM) without serum, however, had a noticeable impact on tantalum oxide. The medium deposited a thin layer on the Pt shield and the gate of the ISFET. During the first day of submersion, this thin layer was impossible to remove with rinsing and ultrasonic baths, and direct contact was needed to scratch the layer. After 4 days in continuous submersion, the layer was so resistant that it could not be removed. It is unknown how exactly this layer was formed or what were the materials it was composed of. However, once the medium was mixed with the FBP serum, the thin layer did not form the tantalum oxide appeared unaffected.

The ISFET that was submerged inside the EMEM, showed a constantly declining output response and would never stabilize, even after days. The drift was so high that an entire unit of pH was lost within a day. Overall, the ISFET was damaged and could not make any reliable detection of the pH of this medium. It is recommended that the ISFET should not be submerged into this medium.

The ISFET was also submerged into the phosphate buffered saline, a buffer solution that used in biological research. The buffer is design to help keep the pH stable. It is composed of potassium phosphate monobasic (KH_2PO_4), sodium chloride (NaCl), and sodium phosphate dibasic ($\text{Na}_2\text{HPO}_4 \cdot 7\text{H}_2\text{O}$). The results of submersion for 18 hours are visible in Figure 26.

The ISFET burn-in was slower inside PBS buffer solution. However, the output stabilized after a drift of 34mV and maintained its stability over hours. According to these results, usage of the ISFET is possible in applications where PBS is used extensively, and it could also be viable for experiments where continuous monitoring is desirable.

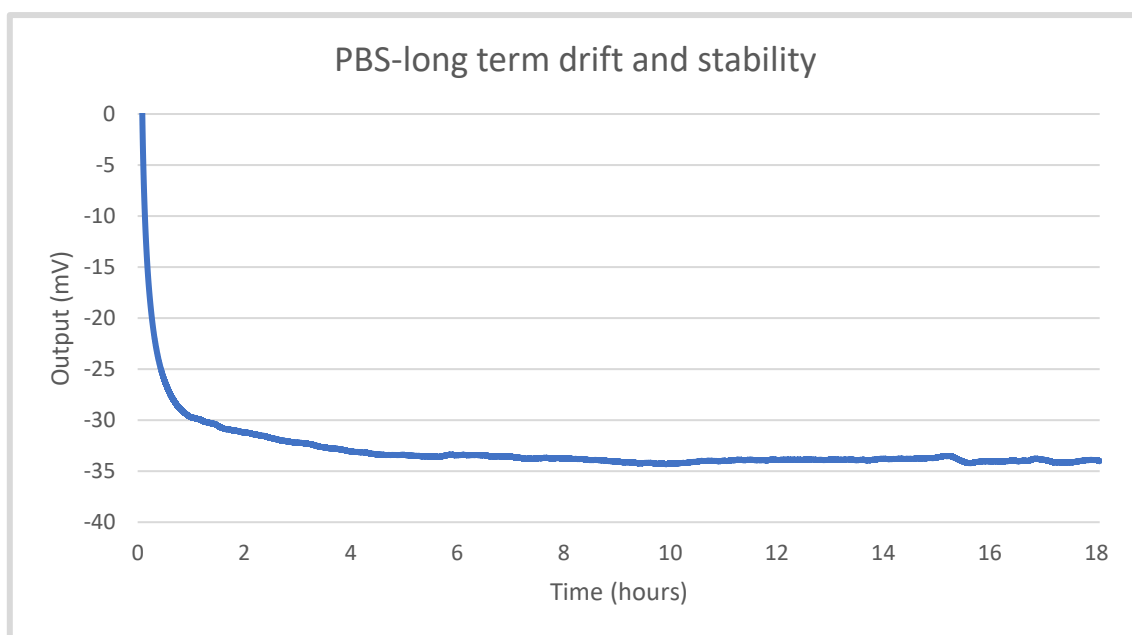


Figure 26: Long-term ISFET response inside PBS (pH 7.4)

6. Sensing Layer with ALD

6.1 Overview of the Gate Structure

The ISFET produced at CSEM has a gate that is constructed by three different stacking layers, shown in Figure 27. The top layer, known as the sensing layer, is the layer that interfaces with the solution. At CSEM it is made from tantalum oxide by the method of LPCVD. The total thickness of the tantalum oxide after the process is around 60nm. Underneath the sensing layer, silicon nitride is deposited using LPCVD at 800°C with 30nm of thickness. Finally, an 80nm silicon oxide is grown using dry oxidation.

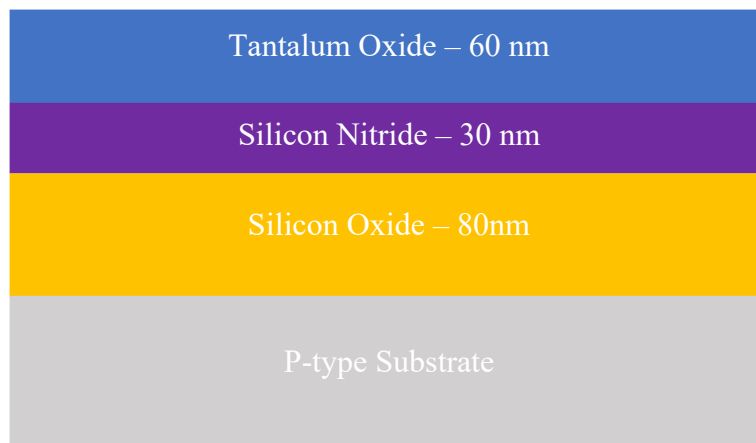


Figure 27 : The gate layers on top of the p-type substrate

Tantalum oxide acts as a good sensing layer since its sensitivity is close to the Nernstian limit. However, while LPCVD was the standard for the deposition process of this material over 20+ years at CSEM, newer technologies, such as atomic layer deposition, which are known for being capable of producing high quality thin layers, were considered as candidates for replacing LPCVD. Hafnium oxide using ALD could also be used as an alternative to tantalum oxide.

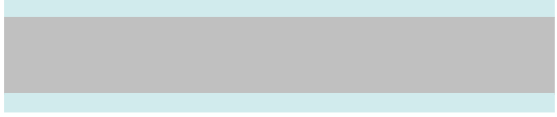
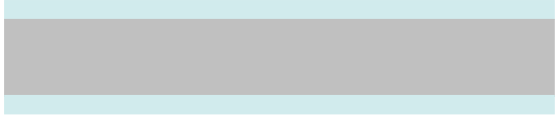





To test these possibilities, an EIS was constructed to evaluate the sensitivity of the hafnium oxide by ALD, all while estimating the corresponding thickness of the hafnium oxide to have equivalence of capacitance. This EIS would be like the one in Figure 27 and kept as close as possible to the gate stack of the ISFET produced by CSEM.


6.2 Construction of the EIS

To construct the EIS, access to the CMi cleanroom at EPFL was granted as well as training on the equipment. The wafers used were p-substrate silicon <100>, with 100mm diameter, 525μm thickness, single side polished with 0.1-0.5 Ohm.cm resistivity, like the ones used for the ISFET production at CSEM.

The EIS was constructed using the following process flow:

Table III: Process Flow of the EIS

Step	Process description	Cross-section after process
01	Substrate: Si Test <i>RCA & Dry Oxidation</i> Machine: <i>Centrotherm</i> Thickness: 80 nm	
02	Annealing Material: <i>Forming gas</i> Temp: 450 °C Time: 30 min.	
03	LPCVD Material: <i>Si3N4</i> Machine: <i>Centrotherm</i> Depth: 30 nm	
04	Spin Coating Material: <i>AZ ECI 3007</i> Machine: <i>ACS200</i> Depth: 1 μm	
05	Backside Removal of Oxide and Si3N4 Machine: <i>STPS APS</i>	
06	Dicing Dimensions: ~3cmx3cm	
07	Resist Removal Material: <i>REMOVER 1165(70°C)</i> Location: <i>Wet Bench</i>	

08	Atomic Layer Deposition Material: HfO_2 Machine: <i>ALD BENEQ</i> Depth: 60 nm	
----	--	--

The RCA, dry oxidation, and annealing (Step 1 and 2) were performed by CMi staff. LPCVD of the silicon nitride was performed at CSEM due to technological incompatibilities and possible cross contamination of equipment at CMi. The resulting thickness of the silicon nitride was ~31.5nm measured by spectroscopic ellipsometry.

The spin coating was performed with a machine by SUSS⁺ Microtech, using a default photoresist material AZ ECI 3007 at 4,5um thickness. The photoresist was applied to perform the dielectric etching using plasma (Step 4) and to protect the wafer during dicing as well. The etching of the silicon nitride and silicon oxide on the backside was performed by the STPS dielectric etcher.

Finally, the wafers are diced, according to specifications and then moved back into the wet bench, where the mask was removed by submerging the chips in 2 subsequent baths of “Remover 1165” at 70°C followed by a “Quick-Dump-Rinse” bath in de-ionized water and a “Cascade” bath in de-ionized water.

The chips are moved into the ALD BENEQ to perform the deposition. The recipe which was used for the hafnium oxide was the following:

- TEMAHf at 80°C as the first precursor
- H₂O at room temperature
- Chamber temperature at 200°C
- 600 cycles are required for the growth of 58.5nm (1 Å/cycle)

The term “cycle” in context is used to describe the deposition mechanism. Each cycle contains four steps repeating in a loop:

1. The TEMAHf is pulsed inside the chamber. Chemisorption takes places on the surface of the exposed layer, in this case the silicon nitride, to form a monolayer.
2. Inert gas (N₂) is used to remove the excess of the TEMAHf from the chamber.
3. H₂O is then pulsed in the chamber, which reacts with the monolayer of TEMAHf.
4. Inert gas (N₂) is once again used to remove the excess of the H₂O from the chamber.

To improve the quality of the deposited hafnium oxide, the ALD machine must be used to grow around 10nm without any substrate, so that the chamber can be thoroughly cleaned before the actual deposition. Otherwise, impurities from previous users may affect the quality. The thickness of the deposited layers was measured using a SOPRA GES 5E spectroscopic ellipsometer. For the measurement to be more precise, a small piece from a test wafer containing only a substrate of silicon was put inside the ALD chamber. The results showed that the hafnium oxide had a thickness of ~58.5nm, and that the oxide underneath had a thickness of ~79nm with ~1nm of variance.

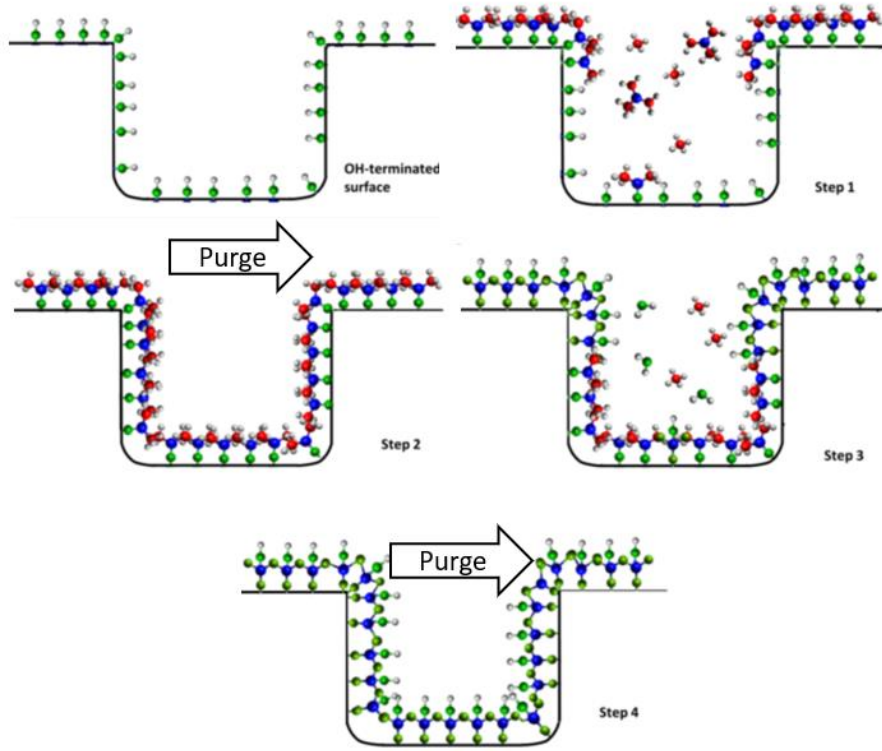


Figure 28: Overview of the ALD process [10].

Rapid thermal annealing was not applied to the chips after the ALD, since it has been found that rapid thermal treatment will decrease capacitance of the hafnium oxide [19]. However, it was discovered that the hysteresis was lower and in general there was an increase in electrical stability. In this instance, the thickness is large enough that leakage current due to loss of capacitance should not be much of an issue.

If annealing must be performed, the recommendation would be that the annealing temperature should match the highest temperature required in the subsequent steps of process flow of the ISFET after the deposition of the gate sensing layer.

The gate capacitance in a MOSFET and the ISFET can be described as a parallel plate capacitor. Typically, in a MOSFET containing a single dielectric the capacitance is described by:

$$C = \frac{\kappa \epsilon_0 A}{t} \quad (6)$$

where: κ is the relative dielectric constant, ϵ_0 is the vacuum permittivity, A as the surface area of the capacitor and t is the thickness of the dielectric material.

However, due to the presence of multiple stacked layers on the gate, the capacitance model of the EIS is the following:

$$\frac{1}{C_{ox}} = \frac{t_{SiO2}}{\kappa_{SiO2} \epsilon_0 A} + \frac{t_{Si3N4}}{\kappa_{Si3N4} \epsilon_0 A} + \frac{t_{HfO2}}{\kappa_{HfO2} \epsilon_0 A} \quad (7)$$

where the first term describes the capacitance of the silicon oxide, the second term describes the capacitance of the silicon nitride interlayer and the third term describes the capacitance due to the hafnium oxide.

6.3 Characterization

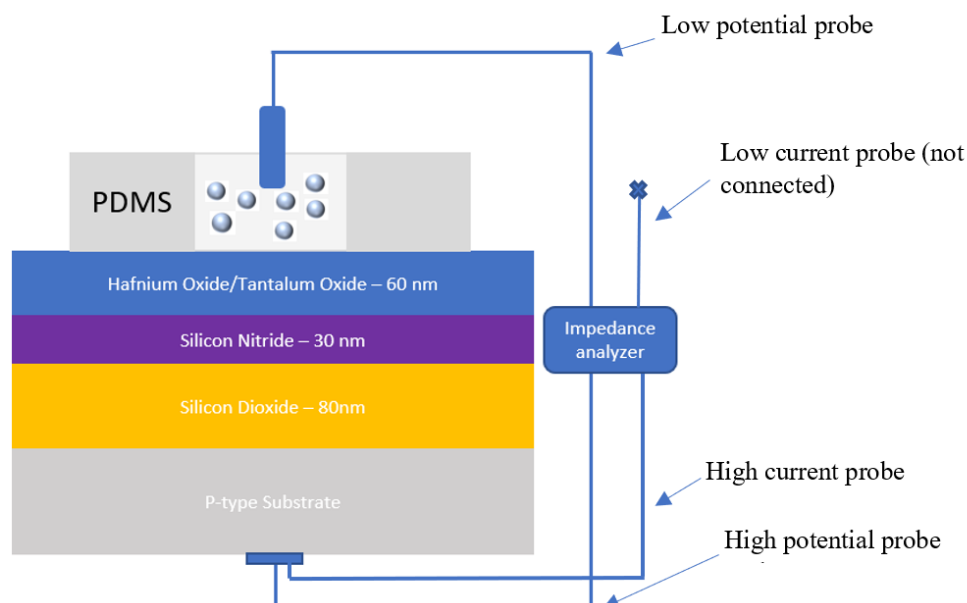


Figure 29: Overview of the EIS measurement setup

The equipment selected to make the CV measurements of the EIS was an LCR precision bridge. In order to perform capacitance measurements, this machine requires four connections, a pair of high potential and high current probes and another pair low potential and low current probes.

The tests were performed under 2kHz frequency with 10ms between each measurement. Lower or quasi-static frequency measurements were impossible as the lab was lacking the necessary equipment for lower frequencies as the results collected were too noisy to extract any meaningful conclusions. The high potential and high current probes were connected on the chuck of the probe station that was in contact with the conductive silicon p-layer of the EIS. From the side of the reference electrode, only the low potential probe was connected to the reference electrode. The capacitance extracted by the measurements is not indicative of the capacitance across the gate stacks, as there is no top electrode adjacent to the tantalum oxide for the LCR bridge to connect to (Figure 29). With this configuration, the values of the capacitance extracted by the instrument can be plotted onto a CV curve. While the values of the capacitance are not correct, repeating the measurements with a different pH will still produce a shift in the CV curve.

The CV curves were extracted with a MATLAB script. To extract the sensitivity, a capacitance point was selected as reference from the linear region of the CV curve. By finding the intersecting points in the pH 4.21 and pH 9.01 curves, the sensitivity is estimated (Figure 30).

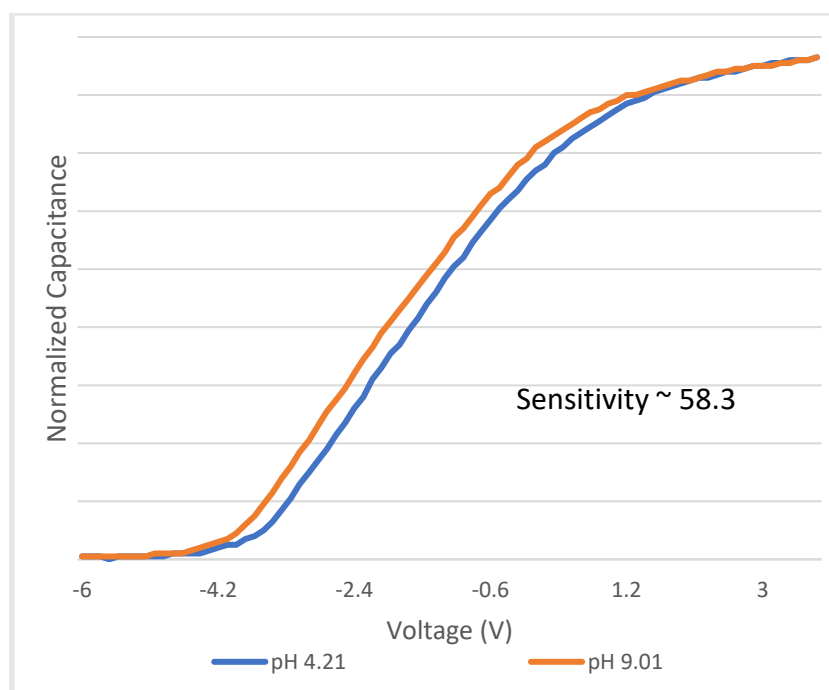


Figure 30: CV measurement of the EIS using hafnium oxide as the sensing layer across two pH solutions.

7. Ion-Selective Membrane

7.1 Overview

Outside of hydrogen ion sensing, many other sensors have been developed aimed at detecting different ions in an aqueous solution. To achieve sensing of a specific ion, the sensor must ignore all other ion activities in the solution. For example, for the ISFET to function properly, it must detect hydrogen ion concentrations while retaining high specificity. A layer that achieves this, allowing only a certain type of ion to pass through its structure, is called “ion-selective membrane”. One of the ways this is achieved is by using a reference electrode with an ion-selective electrode and measuring the difference in potential between the two inside the same solution. Once again, depending on the ion, the maximum potential difference between the solutions containing the targeted ion in different concentrations is limited by the Nernst equation for that specific ion.

Ion-selective membranes are usually composed of different materials: A supporting material, a plasticizer, a counter ion and the ionophore. The ionophore is the material that is responsible for the ion selectivity. The ionophore reversibly immobilizes the ion and either transports it through the membrane with carrier ionophores or creates a channel through which the ion is transported [26].

An ion-selective membrane can be deposited on top of the gate of the ISFET and serve the same function as an ion-selective electrode. In this section the viability of using CSEM ISFET as devices for ion-selective was investigated.

7.2 Aerosol Jet Printing

In this instance, Optomec’s Aerosol Jet Printing tool was used to deposit the ion-selective membranes on the gate of the ISFET. The results are visible in Figure 32. The printer achieves this level of accuracy by first preparing the ink inside a pneumatic atomizer which creates a mist of droplets loaded with the material. These droplets have a size between 1 to 5 microns in diameter. The mist moves from the atomizer chamber through the virtual impactor, where excess gas is removed. Finally, it exits through the deposition head, where it is focused aerodynamically using a stealth gas. Using this technique, the user has precise control over the deposition accuracy as well as the deposition rate of the material [12]. Early into the experiments it was found that the adhesion of the layer was too weak, causing the deposited material to detach. In order to improve adhesion, oxygen plasma treatment was performed on the ISFET, followed by (3-aminopropyl)triethoxysilane (APTES) treatment. The deposition took place after this treatment. No detaching occurred after the APTES treatment. However, there is a possibility that adhesion is not complete, and the solution might still leak under the deposited mass between the ISFET/ion-selective membrane interface.

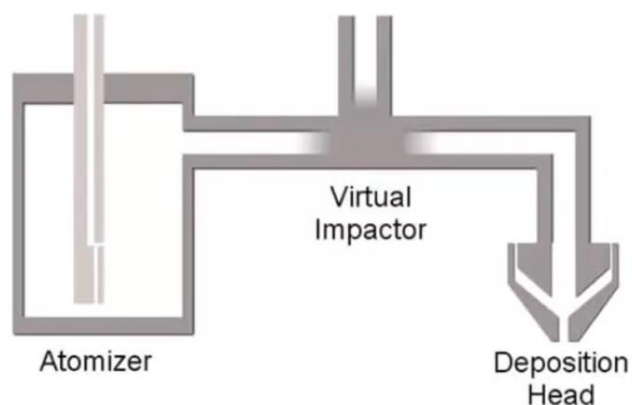


Figure 31: Aerosol Jet Printer process schematic [11].

The ion selective membranes for potassium used in the Aerosol Jet Printing tool was composed of:

- Polyvinyl chloride (PVC)
- Dioctyl sebacate as the plasticizer
- Ionophore (proprietary)
- Potassium tetrakis(4-chlorophenyl) borate (KTCPB)

The ion selective membranes for sodium used in the Aerosol Jet Printing tool was composed of:

- Polyvinyl Chloride (PVC)
- Dioctyl sebacate as the plasticizer
- Ionophore (proprietary)
- Sodium tetrakis[3.5-bis(trifluoromethyl)phenyl]borate (NaTFPB)

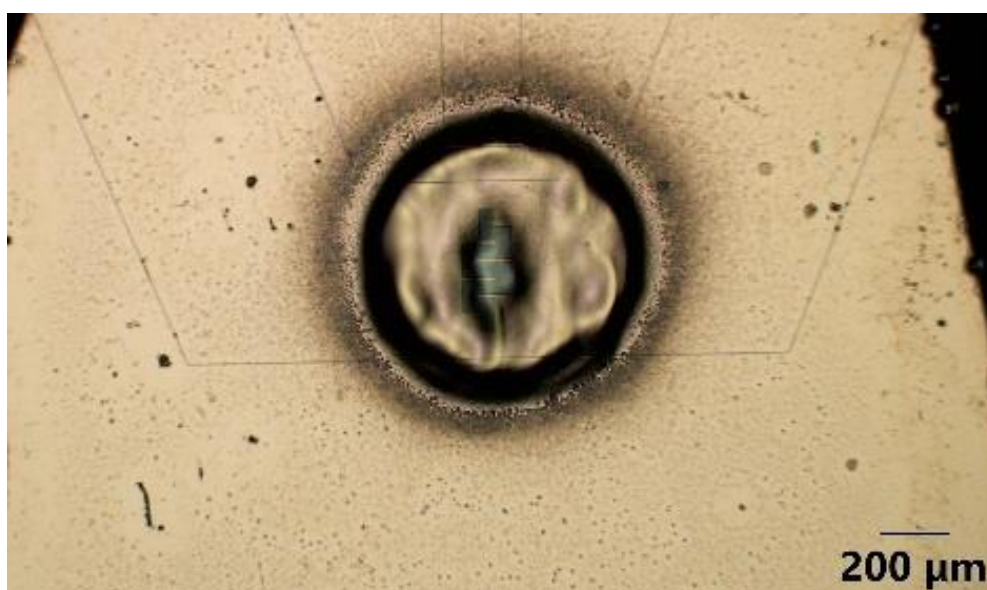


Figure 32: The ISFET after the deposition of the ion-selective membrane using the Aerosol Jet Printer instrument.

7.3 Results

The measurement setup was the same setup used for detecting pH as described in section 4.1. The ISFET could detect concentrations down to 1×10^{-5} M. Further than this value, a significant amount of interference was caused due to the low amounts of the concentration. For potassium ion measurements, the reference electrode was also contaminating the solution slowly, as described in section 2.3. Measurements above 1×10^{-5} M proved to be relatively stable. Cross-contamination between the solutions with different concentrations also proved to be an issue. For this reason, all measurements were done from low concentration to high concentration, and the sensor was thoroughly cleaned multiple times between each test. The ion selective membrane coated ISFET proved capable of detecting different levels of potassium and sodium ions in the solutions. However, the measurements were noisy, with repeated measurements showing a deviation of ~ 8 mV for the same concentration through repeated tests. Figure 33 shows the sensitivity curves for sodium and for potassium ions. It is unknown how much of this deviation is caused due to contamination or due to faults in the deposition method, which could allow the solution to creep under the deposited membrane and produce a mixed signal.

Further experimentation with deposition thicknesses is needed to evaluate the ideal parameters for the Aerosol Jet Printing tool. However, these results show promise that CSEM ISFETs can be used as a sensing transducer for different ions than hydrogen.

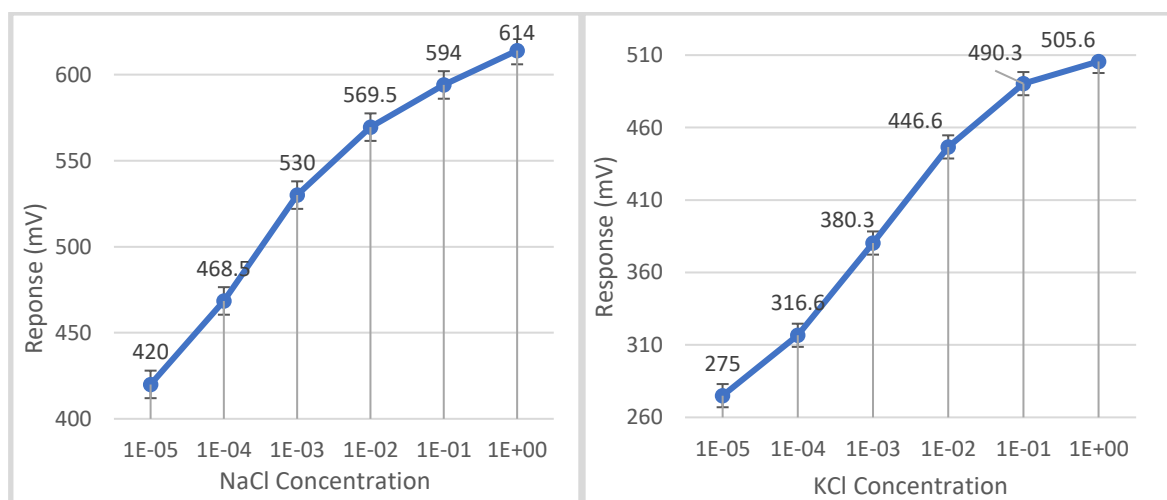


Figure 33: The sensitivity curves for sodium ions (left) and for potassium ions (right).

8. Conclusions

The objective of this report was the characterization of the ISFET produced at CSEM, the investigation of possible improvements in the process flow, and its possible application in the field of ion-selectivity. The first part of the report presented the nature of the problem and its working principles. The second part focused on developing a packaging methodology and the third focused on characterization. The fourth part explored the viability of the ISFET to function in cell culture environments. The fifth part focused on developing an EIS to evaluate ALD as a possible replacement for the already established deposition technique. Finally, in the last part, the possibility of the ISFET working as an ion-selective device was evaluated. The sensor overall proved to be reliable and versatile, however, it was too sensitive to temperature variations under the operating drain current. ALD shows promise as a viable alternative deposition technique but more research is required to have a definitive answer. The ISFET showed that it is not viable for usage in certain cell cultures as the contents of the solutions degraded the performance. Lastly, ion-selective experiments using the ISFETs show that it can be used as a reliable sensor for sensing potassium and sodium ions, however, the specificity and long-term adhesion need to also be evaluated.

9. Bibliography

- [1] Sorensen, S. P. (1909). On the measurement and the importance of hydrogen ion concentration during enzymatic processes. *Biochemische Zeitschrift*, 131-304.
- [2] Walter Boron, F. B. (2004). A cellular and Molecular Approach. *Medical Physiology*.
- [3] Society, R. (2005). Ocean acidification due to increasing atmospheric carbon dioxide.
- [4] <https://www.epfl.ch/research/facilities/cmi/organisation/access-security-in-the-cleanroom/how-to-access-cmi-cleanrooms/>
- [5] Bergveld, P. (1970). Developement of an Ion-Sensitive Solid-State Device for Neurophysiological Measurements. *IEEE Transactions on Biomedical Engineering*, 70-71.
- [6] Bergveld, P. (2003). Thirty years of ISFETOLOGY. What happened in the past 30 years and what may happen in the next 30 years. *Sensors and Actuators B* 88, 1-20.
- [7] Retrieved from CSEM.ch. (2021)
- [8] Retrieved from EPFL.ch. (2021).
- [9] Retrieved from EPFL.ch/research/facilities/CMi. (2021).
- [10] Véronique Cremers, R. L. (2019). Conformality in atomic layer deposition: Current status overview of analysis and modelling. *Applied Physics Reviews* 6.
- [11] <https://optomec.com/printed-electronics/aerosol-jet-technology/>. (2021). Retrieved from <https://optomec.com>.
- [12] Molitch-Hou, M. (2016). Aerosol Jet 5x printer. Retrieved from Engineering.com.
- [13] H. Abe, M. Esashi, & T. Matsuo. (1979). "ISFET's using inorganic gate thin films," in *IEEE Transactions on Electron Devices*, vol. 26, no. 12, pp. 1939-1944, doi: 10.1109/T-ED.1979.19799.
- [14] <https://en.wikipedia.org/wiki/ISFET>. (n.d.).
- [15] Jitty Jose, A. R. (2016). Study of Temperature Dependency on MOSFET Parameter using. *International Research Journal of Engineering and Technology*, vol. 3, Issue 07, 1530-1533.
- [16] Johnson, R. W., Hultqvist, A., & Bent, S. F. (2014). A brief review of atomic layer deposition: from fundamentals to applications. *Materials Today*.
- [17] Lai, C.-S. &.-M.-F. (2006). pH Sensitivity Improvement on 8 nm Thick Hafnium Oxide by Post Deposition Annealing. *Electrochemical and Solid State Letters - ELECTROCHEM SOLID STATE LETT.* 9. 10.1149/1.2163550.

- [18] Shinwari, W. M., Deen, J., & Landheer, D. (2007). Study of the electrolyte-insulator-semiconductor field-effect transistor (EISFET) with applications in biosensor design. *Microelectronics Reliability*, Volume 47, Issue 12. doi:<https://doi.org/10.1016/j.microrel.2006.10.003>
- [19] Rigante, S. (2014). High-K Dielectric FinFETs on Si-Bulk for Ionic and Biological Sensing Integrated Circuits. Lausanne, EPFL. doi:10.5075/epfl-thesis-6134
- [20] P. R. Barabash, R. S. C. Cobbold, & W. B. Wlodarski. (1987, June). Analysis of the threshold voltage and its temperature dependence in electrolyte-insulator-semiconductor field-effect transistors (EISFET's). *IEEE Transactions on Electron Devices*, vol. 34, no. 6, pp. 1271-1282. doi:10.1109/T-ED.1987.23081
- [21] Ravichandran, S., Thiagarajan, C., & Kumar, P. S. (2021). "pH Sensitivity Estimation in Potentiometric Metal Oxide pH Sensors Using the Principle of Invariance", *International Journal of Chemical Engineering*, vol. 2021, Article ID 5551259, 18 pages.
- [22] V. Berland, A. T.-N.-.. (1991). Effect of X-ray radiation on MOSFET's (SIMOX) LF excess noise. RADECS 91 First European Conference on Radiation and its Effects on Devices and Systems, 159-163.
- [23] van der Wal et al, P. (2004). High-k dielectrics for use as ISFET gate oxides. *SENSORS*, 2004 IEEE, vol. 2, pp. 677-680. doi:doi: 10.1109/ICSENS.2004.1426257
- [24] Walter Boron, F. B. (2004). A cellular and Molecular Approach. *Medical Physiology*.
- [25] Yates, D. E., Levine, S., & Healy, T. W. (1974). Site-binding model of the electrical double layer at the oxide/water interface. *J. Chem. Soc, Faraday Trans. 70*, pages 1807–1818. doi:<https://doi.org/10.1039/F19747001807>
- [26] Deneikah T. Jackson, P. N. (2019). Preparation and properties of some ion selective membranes: A review. *Journal of Molecular Structure*, 241-259.
- [27] P. R. Barabash, R. S. (1987). Analysis of the threshold voltage and its temperature dependence in electrolyte-insulator-semiconductor field-effect transistors (EISFET's). *IEEE Transactions on Electron Devices*, vol. 34, no. 6, 1271-1282.

Annex

Description of Sites

➤ EPFL

EPFL is a public research university based in Lausanne, Switzerland founded in 1969. It has over 16.000 students and collaborators and over 370 laboratories. EPFL missions are driven by three core areas [8]:

- Education
- Research
- Technology transfer to industry

EPFL is host to the “Center of MicroNanoTechnology (CMi)” that operates and is regulated from the EPFL core facilities. It is located inside the EPFL campus. CMi offers its users access to a wide variety of machines purposed for the fabrication and characterization of micro and nanotechnologies, as well as education and training by the personnel working at CMi.

- More than 100 different instruments for the construction and research of microtechnologies. These include lithography, etching, thin film deposition, metrology, packaging, and more.
- 1400m² of cleanroom from ISO 5 to ISO 7

CMi is composed of several platforms and two cleanrooms that users occupy. The lower cleanroom is composed of multiple rooms of ISO 5/Class 100, according to the requirements of the equipment within. The upper floor contains several ISO 6 and ISO 7 Zone 4 which contained the atomic layer deposition equipment which was crucial for developing the sensing layers. cleanrooms and are connected with the lower levels by an elevator [9]. During this project, there was an extensive usage of the equipment of the lower floor (BM -1), and in particular.

As CMi is not equipped with characterization instruments apart from microscopy a different laboratory was used to evaluate the microfabricated devices. Characterization of the devices constructed at CMi took place at the “Laboratory of Micro/Nanoelectronic Devices” (NANOLAB), which is located at ELB 217 once again inside the EPFL campus. It is founded and directed by Adrian M. Ionescu. All activities within CMi were under the billing address of NANOLAB for the duration of the project.



Figure 34: Top view of the CMi cleanrooms [4]

Project Schedule (Gantt Diagram)

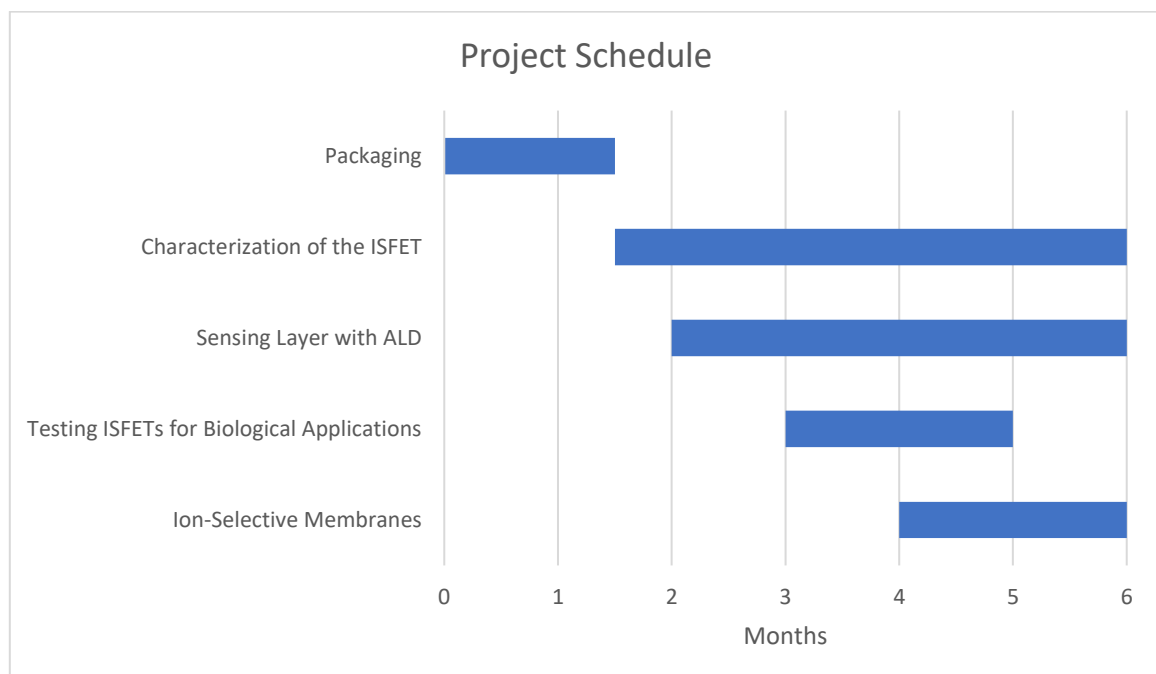


Figure 35: Project overview in Gantt chart format.

Summary

Ion-sensitive field-effect transistors, in addition to glass electrodes and other pH meters, are widely used today as sensors for detecting hydrogen ion concentrations in aqueous solutions. Their usefulness ranges from food applications, to environmental research to the biological and health sectors. This report outlines the procedure of packaging and the characterization results of the ISFET developed at the Swiss Center for Electronics and Microtechnology (CSEM), along with their compatibility with sterilization methods and functioning in cell cultures. An evaluation of atomic layer deposition for forming the sensing layer of the ISFET using an electrolyte-insulator-semiconductor device developed at Center of MicroNanoTechnology and characterized at NANOLAB at École Polytechnique Fédérale de Lausanne. Lastly, using the Aerosol Jet Printing tool, the ISFET was modified into an ion-selective device for potassium and sodium ions and its adhesion and sensing properties were evaluated.

Le transistor à effets de champs activées par ions (ISFET), de la même manière que l'électrodes en verre ou le pH mètre, est largement utilisé pour mesurer la concentration en ion hydrogène des solutions aqueuses. Son champ d'application s'étend de l'agronomie, de la biologie à la santé et à la recherche dans environnement. Ce rapport expose les procédés de packaging et les résultats de caractérisations des ISFET produits au centre suisse pour l'électronique et les micro-technologies (CSEM). Il est également sujet des leurs intégration dans des pétri de cultures nécessitants des méthodes spécifiques de stérilisation. Afin de fonctionnaliser la surface de l'ISFET, La déposition par couches atomiques est expérimentée avec l'utilisation d'un système semiconducteur-isolant-électrolyte développé au centre de MicroNano technologies et caractérisé au NANOLAB à l'Ecole Polytechnique Fédérale de Lausanne. Finalement, l'impression par jet d'aérosol transforme l'ISFET en capteur discriminant les ion potassium et sodium. Ses performances sont ici présentées.

Gli ISFET (Ion-sensitive field-effect transistors), oltre che come elettrodi a vetro e misuratori di pH, sono comunemente usati come sensori di concentrazione di ioni idrogeno in soluzioni acquose. La loro utilità spazia dalle applicazioni nella nutrizione, ricerca ambientale, fino ai settori biologici e medici. Questo report va a evidenziare le procedure di incapsulamento (packaging) e i risultati della caratterizzazione di un ISFET sviluppato al Swiss Center for Electronics and Microtechnology (CSEM), insieme alla sua compatibilità con metodi di sterilizzazione e funzionamento nelle colture cellulari. Un'analisi della deposizione di layer atomici per creare il layer sensibile dell'ISFET usando un dispositivo elettrolita-isolante-semiconduttore sviluppato al Center of MicroNanoTechnology e caratterizzato al NANOLAB dell'École Polytechnique Fédérale de Lausanne. Infine, usando l'Aerosol Jet Printing, l'ISFET è stato trasformato in un dispositivo selettivo rispetto agli ioni potassio e sodio, e ne sono state misurate le sue proprietà di adesione e sensibilità.